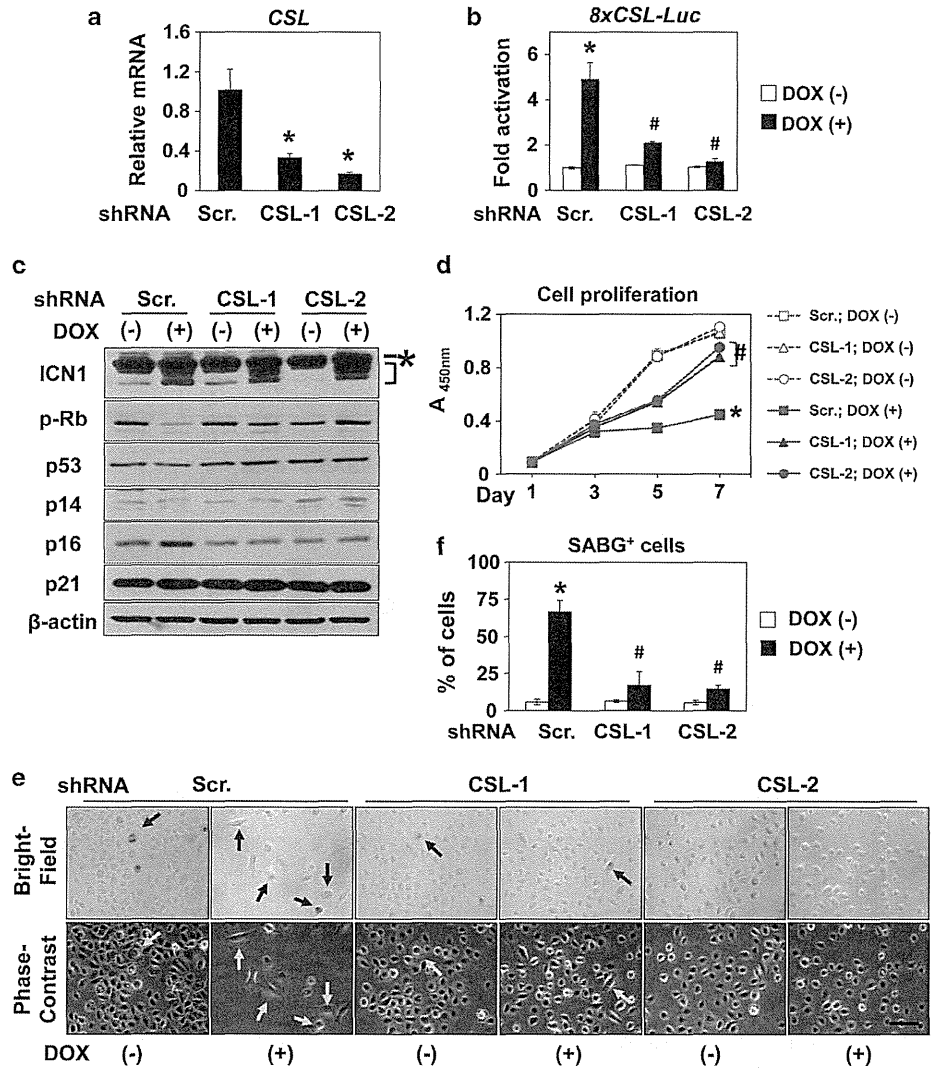

Figure 3. CSL knockdown inhibits ICN1-mediated senescence in EPC2-hTERT cells. EPC2-hTERT carrying *ICN1*$^{Tet\text{-}On}$ was stably transduced with lentivirus expressing two independent short hairpin RNA (shRNA) sequences directed against CSL (CSL-1 and CSL-2) or a non-silencing control scramble shRNA (Scr.) sequence. In panel (**b**), cells were transiently transfected with *8xCSL-luc* 24 h before DOX treatment. Cells were treated with DOX at a concentration of 0 μg/ml [DOX (−)] or 1 μg/ml [DOX (+)] to induce ICN1 for 48 h in panel (**b**) and 7 days in panels (**c**–**f**). Cells were harvested at the indicated time points in panel (**d**). Following DOX treatment, cells were subjected to quantitative RT–PCR for *CSL* mRNA in panel (**a**); luciferase assays for *8xCSL-luc* reporter activity in panel (**b**); western blotting for ICN1, phospho-Rb^{S780} (p-Rb), p53 and cell-cycle regulators in panel (**c**); WST1 assays for cell proliferation in panel (**d**); and SABG assays in panels (**e**) and (**f**). In panel (**a**), β-actin served as an internal control. *$P < 0.05$ vs Scr. ($n = 3$). In panel (**b**), *$P < 0.05$ vs Scr. and DOX (−); #$P < 0.05$ vs Scr. and DOX (+); $n = 3$. In panel (**c**), β-actin served as a loading control. *Denotes transmembrane/intracellular region of endogenous Notch1. Bracket indicates lentivirally expressed ICN1 induced by DOX. In panel (**d**), *$P < 0.05$ vs Scr. and DOX (−) at day 7; #$P < 0.05$ vs Scr. and DOX (+) at day 7; $n = 6$. In panel (**e**), representative bright-field and phase-contrast images of SABG-positive cells with flat and enlarged cell morphology (arrows) as scored in panel (**e**); *$P < 0.05$ vs Scr. and DOX (−); #$P < 0.05$ vs Scr. and DOX (+); $n = 6$.

p16^{INK4A} (Figures 5e and f; Supplementary Figure S11), suggesting that endogenous Notch1 and p16^{INK4A} may cooperate to mediate senescence when p16^{INK4A} becomes accessible to Rb as a consequence of E7 knockdown.

E7 suppresses TGF-β signaling by blocking Smad3 binding to target sequences on DNA.[41] As TGF-β induces the Notch ligand JAG1 in keratinocytes,[42] we suspected that RNAi directed against HPV gene products may reactivate TGF-β signaling to allow Notch activation via JAG1. In agreement, TGF-β target genes *PAI1* and *JAG1* were found to be elevated in the presence of E7 siRNA (Figures 5b and g). Moreover, E7 knockdown resulted in the activation of both TGF-β and Notch reporter constructs in transfection assays (Figure 5h). Finally, E7 knockdown led to upregulation of Notch1 mRNA (Figure 5g). These data agree with Notch1 suppression in HPV-transformed cells.[19] Therefore, HPV E6/E7 may suppress TGF-β signaling to inhibit the Notch1-mediated senescence program.

Endogenous Notch1 mediates senescence in non-transformed keratinocytes in response to TGF-β stimulation

Next, we asked whether and how TGF-β may induce senescence via Notch1 in cells without HPV oncogene products. As the majority of transformed human esophageal cells resist senescence in response to TGF-β stimulation,[7] we used non-transformed EPC2-hTERT cells. TGF-β induced JAG1 to enhance endogenous

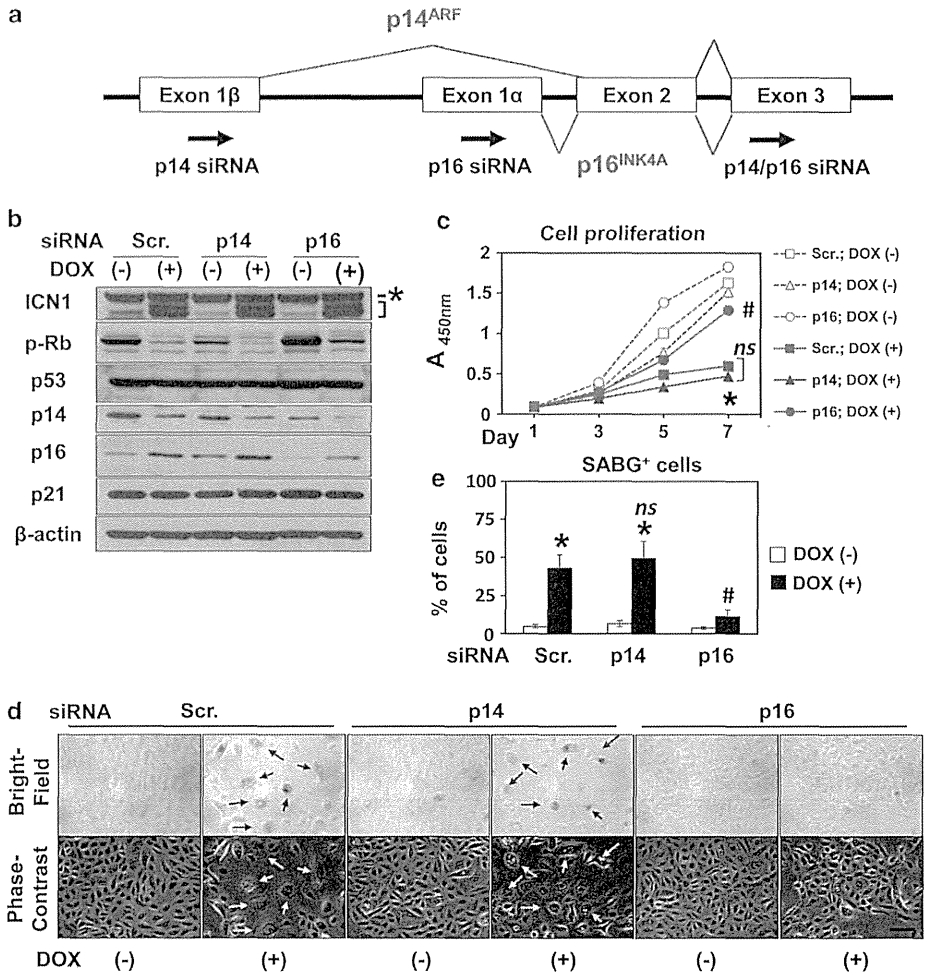

Figure 4. p16^{INK4A} may contribute to ICN1-induced senescence in EPC2-T cells. In panel (**a**), siRNA was designed to target *p14^{ARF}* (p14 siRNA) and *p16^{INK4A}* (p16 siRNA) on the *INK4A* locus. p14/p16 siRNA was used to knockdown *p14^{ARF}* and *p16^{INK4A}* concurrently as shown in Supplementary Figure S8. In panels (**b**–**e**), EPC2-T carrying *ICN1^{Tet-On}* was treated with 0 μg/ml [DOX (−)] or 1 μg/ml [DOX (+)] of DOX to induce ICN1 following transfection with p14 siRNA, p16 siRNA or a non-silencing control scramble short interfering RNA (Scr.). Starting 24 h after transfection, cells were treated with DOX for 7 days in panels (**b**), (**d**) and (**e**) and at the indicated time points in panel (**c**) and subjected to western blotting for ICN1, phospho-Rb^{S780} (p-Rb), p53 and cell-cycle regulators in panel (**b**); WST1 assays for cell proliferation in panel (**c**); and SABG assays in panels (**d**) and (**e**). In panel (**b**), β-actin served as a loading control. *Denotes transmembrane/intracellular region of endogenous Notch1. Bracket indicates lentivirally expressed ICN1 induced by DOX. In panel (**c**), *$P < 0.05$ vs Scr. and DOX (−) at day 7; #$P < 0.05$ vs Scr. and DOX (+) at day 7; NS, not significant vs Scr. and DOX (+) at day 7 ($n = 6$). In panel (**d**), representative bright-field and phase-contrast images of SABG-positive cells with flat and enlarged cell morphology (arrows) as scored in panel (**e**); *$P < 0.05$ vs Scr. and DOX (−); #$P < 0.05$ vs Scr. and DOX (+); NS, not significant vs Scr. and DOX (+); $n = 6$. Note that densitometry from panel (**b**) was summarized along with cell proliferation and SABG data in panels (**c**–**e**) in Supplementary Table S1.

ICN1^{Val1744} expression and activate CSL-dependent transcription, leading to Rb dephosphorylation, inhibition of cell proliferation, G0/G1 cell-cycle arrest and induction of flat and enlarged cell morphology as well as SABG activity (Figures 6a–f; Supplementary Figure S12a). Importantly, GSI inhibited the ability of TGF-β to trigger Notch1 activation, growth inhibition and SABG induction (Figures 6b, c–f; Supplementary Figure S12a), indicating that Notch activation mediates TGF-β-induced senescence. Moreover, RNAi directed against Notch1 decreased significantly TGF-β-induced Notch1 and SABG activation (Figure 6g and Supplementary Figures S12b and c). Nevertheless, GSI or Notch1 knockdown reversed G0/G1 cell-cycle arrest to a partial extent (Figure 6e; and data not shown) as corroborated by the limited antagonistic effect upon Rb dephosphorylation and cell proliferation in the presence of TGF-β (Figures 6b and d; Supplementary Figure S12b). TGF-β induced p16^{INK4A} and p21 before full induction of ICN1^{Val1744} (Figure 6a) although Notch1 knockdown delayed Rb dephosphorylation (Supplementary Figure S12b). Thus TGF-β may not necessarily depend upon Notch to induce cell-cycle arrest but instead may depend largely upon Notch1 for SABG activation in this context. These data suggest that endogenous Notch1 may mediate TGF-β-induced senescence.

Ectopically expressed ICN1 facilitates anchorage-independent cell growth and tumor formation in transformed human esophageal keratinocytes

We explored finally how ICN1 may affect tumorigenicity of transformed cells that are able to negate ICN1-induced senescence. To this end, we first conducted soft agar colony-formation assays using EN60 and TE11 cells with tetracycline-inducible ICN1. ICN1 enhanced colony formation in both cell lines and stimulated

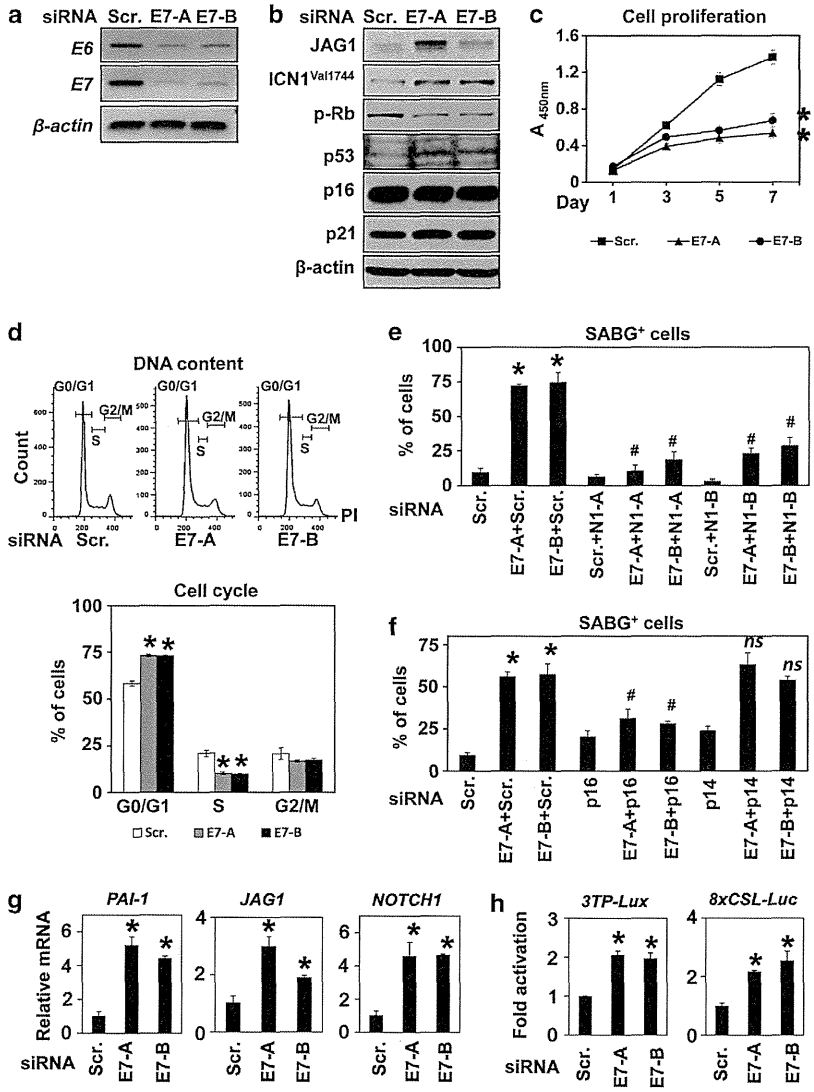

Figure 5. HPV E6/E7 knockdown activates endogenous Notch1 and TGF-β signaling to induce senescence in EN60 cells. EN60 cells expressing HPV E6/E7 were transiently transfected with two independent siRNA sequences directed against either HPV E7 (E7-A and E7-B) or a non-silencing control scramble short interfering RNA (Scr.) along with or without siRNA directed against Notch1 (N1-A and N1-B), $p16^{INK4A}$ (p16) or $p14^{ARF}$ (p14). In panel (**h**), cells were concurrently transfected with the indicated reporter constructs. Cells were analyzed 7 days after transfection by RT–PCR for HPV E6 and E7 transcripts in panel (**a**); western blotting for the indicated molecules in panel (**b**); WST1 assays for cell proliferation in panel (**c**); flow cytometry for cell cycle in panel (**d**); and SABG assays in panels (**e**) and (**f**); quantitative RT–PCR for the indicated mRNA in panel (**g**); and luciferase assays for activation of the TGF-β (3TP-Lux) and Notch (8xCSL-luc) reporters in panel (**h**). In panel (**a**), β-actin served as an internal control. In panel (**b**), β-actin served as a loading control. In panel (**d**), representative histogram plots are shown. Proportions of cells in G0/G1, S and G2/M cell-cycle phases were determined. $^*P < 0.05$ vs Scr.; $n = 3$. In panel (**e**) and (**f**), SABG-positive cells were scored (see Supplementary Figure S11 for representative photomicrographs). $^*P < 0.05$ vs Scr. only; $\#P < 0.05$ vs Scr.+either E7-A or E7-B; NS, not significant vs Scr.+either E7-A or E7-B; $n = 6$ in panels (**e**) and (**f**). In panel (**g**), β-actin served as an internal control. $^*P < 0.05$ vs Scr.; $n = 3$. In panel (**h**), $^*P < 0.05$ vs Scr.; $n = 4$.

colony growth in TE11 but not in EN60 (Figure 7a). Next, we performed xenograft transplantation experiments. In nude mice, ICN1 greatly enhanced tumor growth by EN60 and TE11 cells (Figure 7b). Interestingly, histopathological analysis of xenograft tumors revealed a significantly increased number of less differentiated, smaller and proliferative ESCC cells upon ICN1 expression (Figure 7c and Supplementary Figure S13). These results suggest that in response to Notch1 activation ESCC cells not only negate ICN1-induced senescence but also gain more malignant characteristics, revealing an oncogene-like attribute of ICN1.

DISCUSSION

Notch1 has been implicated in replicative senescence in endothelial cells;[31,32] however, this is the first study demonstrating in epithelial cells that Notch1 activates cellular senescence defined by cell-cycle arrest, morphological changes, SABG induction and molecular changes, including Rb dephosphorylation. Importantly, our study sheds light on the role of cellular senescence checkpoint functions in influencing dichotomous Notch activities in the neoplastic context. Our data indicate that activated Notch1 may induce senescence in concert with intact cell-cycle checkpoint functions (Figures 1–4). When they are fully impaired, cells may

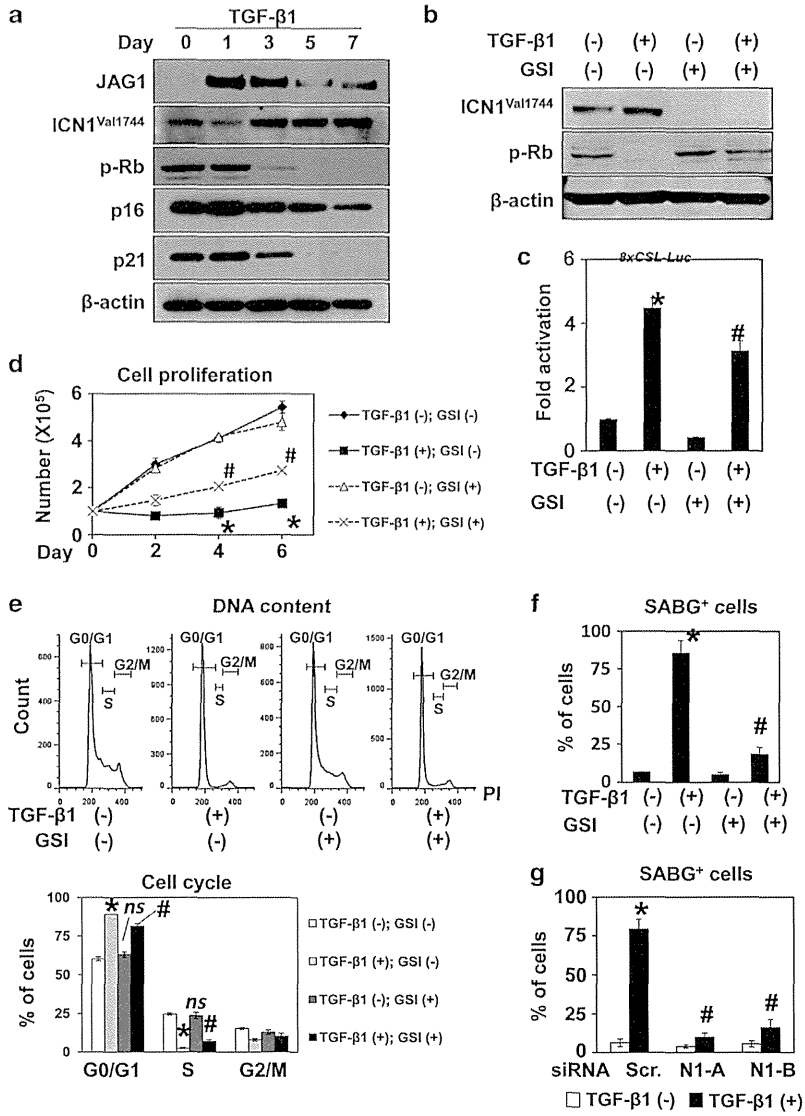

Figure 6. TGF-β stimulates endogenous Notch1 to mediate senescence in EPC2-hTERT cells. EPC2-hTERT cells were stimulated with 5 ng/ml TGF-β1 alone or along with either GSI (1 μM compound E) or DMSO (vehicle) in panels (**a**–**f**). Cells were transiently transfected with a *8xCSL-luc* Notch reporter construct 24 h before TGF-β stimulation in panel (**c**) and siRNA directed against Notch1 (N1-A and N1-B) 24 h before TGF-β stimulation in panel (**g**). Cells were analyzed at the indicated time points in panels (**a**) and (**d**); and 7 days after TGF-β stimulation in panels (**b**), (**c**), (**e**–**g**). Western blotting determined the indicated molecules with β-actin serving as a loading control in panels (**a**) and (**b**). In panel (**c**), luciferase assays determined activation of the *8xCSL-luc* Notch reporter construct. In panel (**d**), the cell number was counted to determine cell proliferation. In panel (**e**), flow cytometry was done to determine cell cycle. In panels (**f**) and (**g**), SABG assays were carried out and scored (see Supplementary Figures S12a and c for representative photomicrographs). In panel (**c**), $^{*}P < 0.05$ vs TGF-β1 (−) and GSI (−); $\#P < 0.05$ vs TGF-β1 (+) and GSI (−); $n = 3$. In panel (**d**), $^{*}P < 0.05$ vs TGF-β1 (−) and GSI (−); $\#P < 0.05$ vs TGF-β1 (+) and GSI (−); $n = 3$. In panel (**e**), representative histogram plots are shown. Histograms show proportions of cells in G0/G1, S and G2/M cell-cycle phases. $^{*}P < 0.05$ vs TGF-β (−) and GSI (−); NS, not significant vs TGF-β (−) and GSI (−); $\#P < 0.05$ vs TGF-β (+) and GSI (−); $n = 3$. In panel (**f**), $^{*}P < 0.05$ vs TGF-β1 (−) and GSI (−); $\#P < 0.05$ vs TGF-β1 (+) and GSI (−); $n = 6$. In panel (**g**), $^{*}P < 0.05$ vs TGF-β1 (−) and Scr. (−); $\#P < 0.05$ vs TGF-β1 (+) and Scr.; $n = 6$.

negate senescence (Supplementary Figure S5) but gain more malignant characteristics in response to Notch1 activation (Figure 7). In this context, Notch1 exhibits features of an oncogene (Figure 8a). However, endogenous Notch1 mediates senescence as a downstream effector for TGF-β signaling (Figure 6). Such a function of Notch1 may be targeted for inactivation by the HPV oncogenes E6 and E7 (Figure 5), implying a feature of Notch1 as a tumor-suppressor gene (Figure 8b). Like TGF-β acting as a tumor suppressor in the early stage of skin carcinogenesis while promoting tumor progression in later states,[43] Notch1 may have differential roles during cancer development and progression.

Notch activity can be influenced by the intensity or duration of ligand stimulation, differential Notch receptor paralogs, ligands and co-existing factors. Hypoxia and TGF-β are essential components in the tumor microenvironment to facilitate invasive growth of ESCC.[44–46] ICN1 interacts with transcription factors such as SMAD3 and HIF-1α.[42,47] Notch1 activates Notch3 to induce squamous-cell differentiation markers, including IVL and KRT13.[13] As KRT13 expression peaked at a lower DOX concentration (Supplementary Figure S1a), a higher Notch activation may be required for senescence. Unlike squamous-cell differentiation, our data suggest that Notch1 may induce senescence independent of

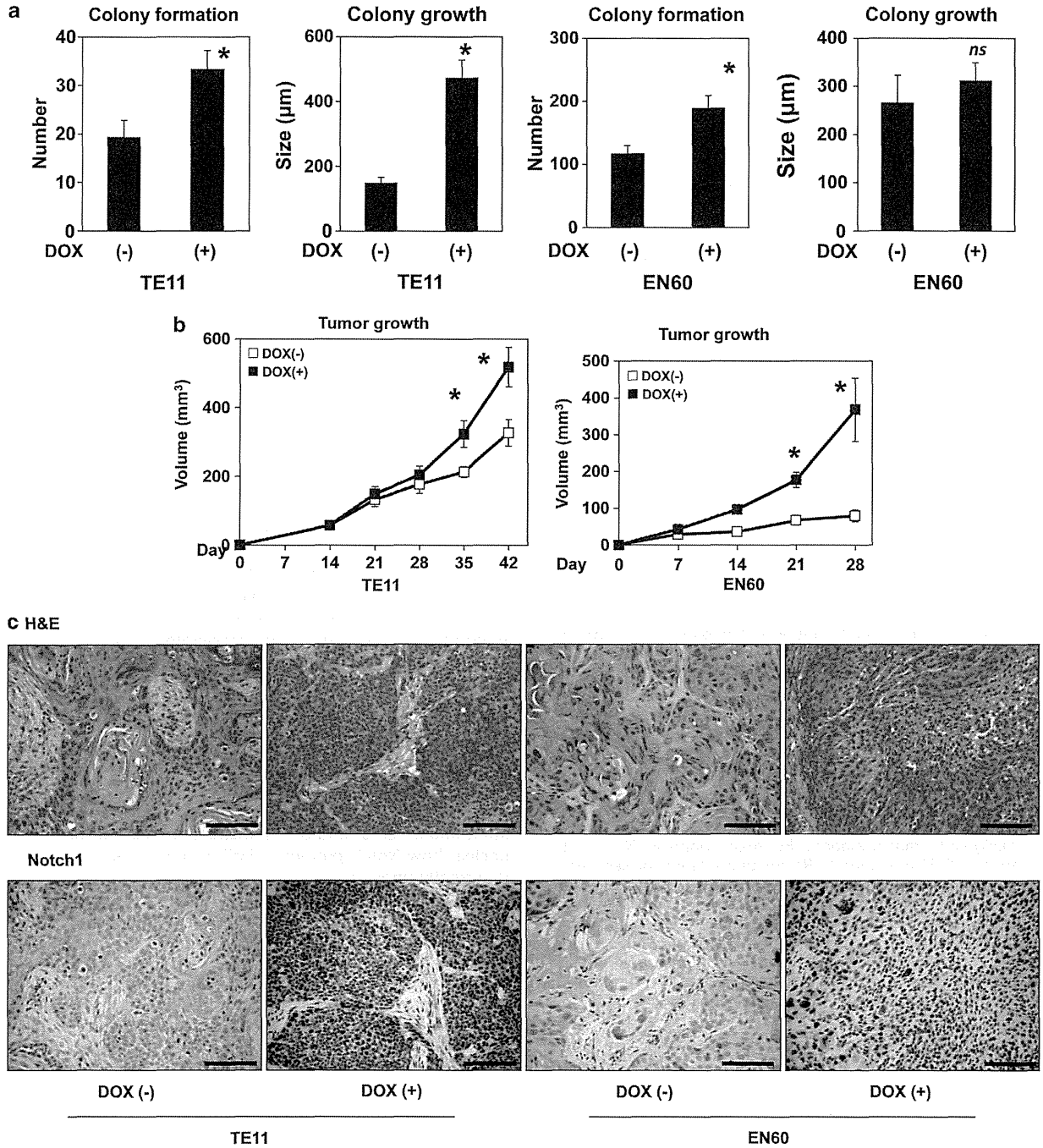

Figure 7. ICN1 increases malignant potentials in esophageal cells negating ICN1-mediated senescence. TE11 and EN60 cells carrying *ICN1*$^{Tet\text{-}On}$ were subjected to soft agar colony-formation assays in panel (**a**) and xenograft transplantation experiments in panels (**b**) and (**c**). In panel (**a**), cells were grown for 2 weeks in soft agar in the presence [DOX (+)] or absence [DOX (−)] of 1 μg/ml DOX and photomicrographed. Colony number and size were determined per low-power field under light microscopy. *$P < 0.01$ vs DOX (−); $n = 6$. In panels (**b**) and (**c**), immunodeficient mice underwent xenograft transplantation and fed with DOX-containing pellets (20 mg/kg) to induce ICN1. Tumor growth was monitored for the indicated time periods in panel (**b**). Representative images for H&E and immunohistochemistry for Notch1 in resulting xenograft tumors are shown in panel (**c**). Note tumors in mice treated with DOX display less-differentiated SCC featuring smaller ESCC cells. Tumors grown in DOX-untreated control mice display well-differentiated SCC with keratin pearl formation. Scale bar = 100 μm.

Notch3 (Supplementary Figure S14). We also confirm a recent report[48] that ectopically expressed ICN3 induces senescence by suppressing Notch1 (Supplementary Figure S15), revealing a redundant role of Notch1 and Notch3 in senescence in epithelial cells.

How does Notch regulate senescence? Cell-cycle arrest can be mediated by p16^{INK4A} and p21. We do not exclude p21, as postulated in Notch3-mediated senescence,[48] although ICN3 did not induce p21 in EPC1-hTERT (Supplementary Figure S15). Our data suggest that the p16^{INK4A}-Rb pathway may have a

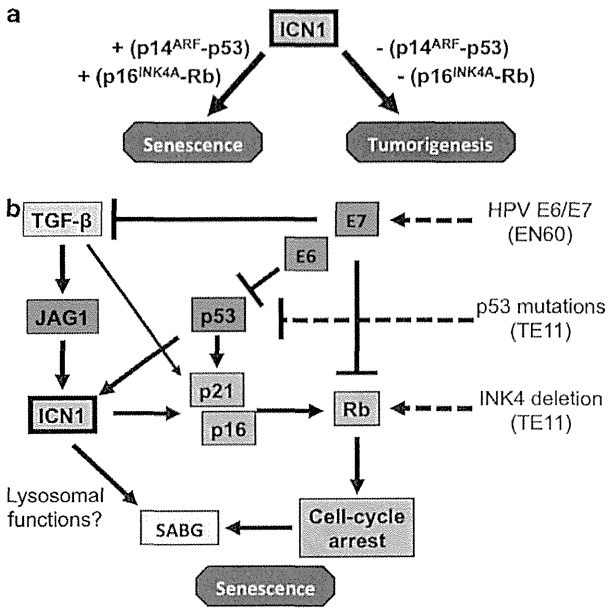

Figure 8. Model: Notch1 displays both oncogene and tumor-suppressor attributes in a context-dependent manner. (**a**) Like classic oncogenes (for example, Ras and Raf), ICN1 induces senescence via intact cell-cycle checkpoint functions. In normal human esophageal keratinocytes, the $p16^{INK4A}$-Rb pathway may have a predominant role in ICN1-induced senescence; however, the $p14^{ARF}$, p53 and others may constitute alternative pathways to mediate senescence when the $p16^{INK4A}$-Rb pathway is impaired. When cell-cycle checkpoint functions are fully impaired (for example, concurrent Rb and p53 inactivation), cells fail to undergo senescence in response to ICN1, resulting in malignant transformation. (**b**) Endogenous Notch1 may serve as a tumor suppressor by mediating TGF-β-induced senescence. TGF-β has been implicated in replicative senescence[50] as well as oncogene-induced senescence.[51,52] TGF-β requires p53 to transactivate p21.[64] Notch1 may be targeted for inactivation by HPV oncogenes E6 and E7 during malignant transformation. E6 may suppress Notch1 by degrading p53.[49] E7 also targets Rb for degradation or sequestration. We find that HPV E6 and E7 inhibit TGF-β signaling to prevent the activation of endogenous Notch1 and induction of $p16^{INK4A}$ and p21. Although TGF-β may induce cyclin-dependent kinase inhibitors independent of Notch1, Notch1 may regulate the SABG activity independent of cell-cycle regulation. As oncogene-induced senescence may involve autophagy and lysosomal functions,[65] Notch signaling may regulate the activity of SABG, a lysosomal enzyme.[66,67]

predominant role in ICN1-induced senescence in normal esophageal keratinocytes expressing $p16^{INK4A}$ (Figure 4, Supplementary Figures S9 and S10); however, complex interplays may exist between multiple cell-cycle regulators (Figure 4, Supplementary Figures S9 and S10; Supplementary Table S1). Given limited RNAi efficiency especially in EPC2-T, $p14^{ARF}$ may not be unequivocally dismissed; however, ICN1 suppressed $p14^{ARF}$ during senescence (Figure 2b) as observed in oncogenic Ras^{G12V}-induced senescence in EPC2-hTERT.[5] The inability of $p53^{R175H}$ to prevent ICN1-induced senescence in EPC2-hTERT (Supplementary Figure S7) also diminished the role of p53. Nevertheless, p53 was upregulated in EPC2 undergoing replicative senescence with concurrent Notch1 activation (Figure 1c). HPV E6 may suppress Notch1 by degrading p53.[38,49] Finally, ICN1 induced senescence in EPC1-hTERT without detectable $p16^{INK4A}$ expression (Supplementary Figure S2). Thus, redundant pathways may allow Notch-induced senescence in cell- and context-dependent manners.

We show for the first time that endogenous Notch1 mediates TGF-β-induced senescence (Figure 6), corroborating a tumor-suppressor function of Notch1 activated in response to TGF-β stimulation. TGF-β signaling is implicated in replicative senescence[50] as well as Ras-induced senescence.[51,52] Concurrent expression of oncogenic Ras and DNMAML1 in human primary keratinocytes resulted in aggressive SCC,[24] suggesting that DNMAML1 may inhibit Notch-mediated senescence activated by Ras during malignant transformation. Besides loss-of-function Notch1 mutations,[20–22] tumor-suppressor activities of Notch have been suggested by Notch downregulation via p53 dysfunction[24,49] and EGFR overexpression.[53] As senescence can be triggered by either oncogene activation or loss of tumor-suppressor functions,[54] Notch suppression may allow these genetic lesions to promote carcinogenesis.

TGF-β also facilitates tumor progression. TGF-β induces JAG1 to activate Notch1 during epithelial–mesenchymal transition (EMT).[42] Thus, Notch activation may contribute to tumor progression stimulated by TGF-β. Besides cancer cell invasion, metastasis and cancer stem cell regulation,[55] EMT may circumvent oncogene-induced senescence.[56] In this context, TGF-β and Notch seem to cooperate to activate EMT but not senescence. What is a molecular mechanism facilitating the conversion of TGF-β and Notch from tumor suppressors to promoters? Transformed human esophageal keratinocytes undergo EMT in response to TGF-β stimulation, negating senescence through transcriptional repression of $p16^{INK4A}$ by ZEB1/2, EMT regulators.[7] Thus a preexisting dysfunctional $p16^{INK4A}$/Rb-mediated cell-cycle regulatory machinery may nullify Notch-mediated senescence in transformed cells. Although our data show an accelerated growth and altered differentiation in tumors expressing ICN1 (Figure 7), ICN1 suppressed tumor growth by oral SCC cell lines carrying loss-of-function Notch1 mutations,[57] where ICN1 induced SABG but not morphological features of senescent cells *in vitro*. ICN3 inhibited tumor growth in cancer cell lines.[48] By contrast, ICN3 induced aggressive inflammatory breast cancer cells when expressed in the mammary stem/progenitor cells in mice.[58] Thus it is possible that ICN1 may have differential roles in different subsets of intratumoral cells and/or premalignant cells. It also remains unclear how Notch promotes EMT in tumors. Such investigation is currently underway.

MATERIALS AND METHODS

Cell lines and treatment

EPC1 and EPC2, normal human esophageal keratinocytes and their derivatives (EPC1-hTERT, EPC2-hTERT, EPC2-T, EPC2-T-GFP and EPC2-T-DNMAML1) as well as EN60 and TE11 cells were described previously.[4,7,35,46] Cells were counted with Countess Automated Cell Counter (Invitrogen, Carlsbad, CA, USA) with 0.2% Trypan Blue dye to exclude dead cells. Population doubling time was determined as described.[3] Cells were treated with 1 μM Compound E, a GSI, or 5 ng/ml TGF-β1 as described.[7,13] Phase-contrast images were acquired using a Nikon Eclipse E600 microscope (Nikon, Tokyo, Japan).

Generation of pTRIPZ-ICN1 and pTRIPZ-ICN3

Platinum *Pfx* DNA polymerase (Invitrogen) was used to amplify cDNAs by PCR for ICN1 (Arg-1761 to Lys-2555 of full-length human Notch1) with primers *Age*I-ICN1 (5′-AGCAGCACCGGTGCCACCATGCGGCGGCAGCATGGC CAGCT-3′) and *Mlu*I-ICN1 (5′-AGCAGCACGCGTTTACTTGAAGGCCTCCGGA ATGCGGG-3′); using MigRI-ICNX[59] as a template, ICN3 (Met-1663 to Ala-2331 of full length human Notch3) with primers *Age*I-ICN3 (5′-AGC AGCACCGGTGCCACCATGGTGGCCCGGCGCAA-3′) and *Mlu*I-ICN3 (5′-AGCAG CACGCGTTCAGGCCAACACTTGCCTCTTG-3′); using pcDNA3.1-ICN3 (a gift of Dr Tao Wang) as a template. Following initial incubation at 94 °C for 5 min, PCR was carried out for 35 cycles at 94 °C for 15 s for denaturing, 56 °C for 30 s for annealing, 68 °C for 3 min for extension, with extended incubation at 68 °C for 5 min after the final extension. The ICN1 and ICN3 PCR products were ligated into the pTRIPZ (Open Biosystems, GE Healthcare, Little

Chalfont, UK) at *Age*I and *Mlu*I sites, replacing the parental sequence flanked by these restriction sites with either cDNA under the tetracycline-inducible promoter, resulting in creation of pTRIPZ-ICN1 and pTRIPZ-ICN3. All constructs were verified by DNA sequencing.

Retrovirus and lentivirus-mediated gene transfer

MigRI-ICNX and MigRI (control vector) were used as described.[13] The lentiviral pTRIPZ-ICN1, pTRIPZ-ICN3 and pGIPZ expressing short hairpin RNA directed against human CSL designated CSL-1 and CSL-2 (clone ID nos. V2LHS_114863 and V2LHS_263385) or a non-silencing scramble sequence (RHS4346) (Open Biosystems) were transfected into HEK-293T cells with Lipofectamine LTX reagent (Invitrogen) to produce replication-incompetent viruses. Stable cell lines were established by drug selection for 7 days with 1 μg/ml of Puromycin (Invitrogen) for pTRIPZ and selected by fluorescence-activated cell sorter for pGIPZ-transduced GFP expressing cells by FACSVantage SE (Becton Dickinson, Franklin Lakes, NJ, USA).

Transient transfection for RNAi and dual-luciferase assays

siRNA directed against Notch1 (N1-A, HSS181550 and N1-B, HSS107249), HPV16 E7 (E7-A, s445412 and E7-B, s445413), *p14/p16* (p14/p16-A, s216 and p14/p16-B, s218), *p14* (5′-GATGCTACTGAGGAGCCAGCG-3′) and *p16* (5′-AACGCACCGAATAGTTACGGT-3′) (Figure 4a), p15 (p15-A,s2843 and p15-B, s2844) or a non-targeting scramble control sequence (4390843, Invitrogen) was transfected using the Lipofectamine RNAiMAX reagent (Invitrogen), following the manufacturer's instructions.

Transient transfection of reporter plasmids and luciferase assays were performed as described previously.[7,13] Briefly, 400 ng of 8xCBF1-luc (designated as *8xCSL-luc*),[60] a Notch-inducible reporter, or p3TP-Lux,[61] a TGF-β-inducible reporter, or pGL3-p16[62] containing a 2.3-kilobase $p16^{INK4A}$ promoter was transfected. Cells were incubated in the presence or absence of 1 μg/ml DOX to induce ICN1 in cells expressing $ICN1^{TetOn}$ for 48 h before cell lysis. Alternatively, 5 ng/ml TGF-β1 was added at 24 h after transfection and incubated for an additional 48 h before cell lysis. The mean of firefly luciferase activity was normalized with the co-transfected Renilla luciferase activity. Transfection was carried out at least three times, and variation between experiments was not $>15\%$.

WST-1 cell proliferation assays

The WST-1 reagent (Roche, Basel, Switzerland) was used for colorimetric cell proliferation assays following the manufacturer's instructions. All experiments were performed in sextuplicate.

SABG assays

The Senescence β-Galactosidase Staining Kit (Cell Signaling, Danvers, MA, USA) was used to stain senescent cells, which were scored by counting at least 100 cells high-power field ($n=3$–6) under light microscopy.

Cell-cycle analysis

Cellular DNA content was determined by flow cytometry. In brief, cells were fixed with 70% ethanol at −20 °C, washed twice with phosphate-buffered saline and incubated with 50 μg/ml propidium iodide and 200 μg/ml RNase A for 30 min at room temperature. At least 10 000 events were recorded and analyzed by FACSCalibur (BD Biosciences, San Jose, CA, USA) with the FlowJo software (Tree Star, Ashland, OR, USA).

RNA isolation, cDNA synthesis and real-time reverse transcriptase–PCR (RT–PCR)

RNA extraction and cDNA synthesis were done as described.[13,35] Real-time RT–PCR was done with SYBR Green and TaqMan Gene Expression Assays (Applied Biosystems, Foster City, CA, USA) for NOTCH1 (Hs01062014_m1), NOTCH3 (Hs00166432_m1), IVL (Hs00846307_s1), CK13 (Hs00999762_m1), CSL (Hs01068138_m1), JAG1 (Hs00164982_m1), HES5 (Hs01387463_g1), HES1(Hs00172878_m1), HEY1 (Hs00232618_m1), HEY2 (Hs00232622_m1), CDKN2A/$p16^{INK4a}$ (Hs99999189_m1), CDKN2B/$p15^{INK4b}$ (Hs00394703_m1), CDKN1A/p21 (Hs00355782_m1), CDKN1B/p27 (Hs00153277_m1), CDKN1C/p57 (Hs00175938_m1) and PAI-1 (Hs01126606_m1) using the StepOnePlus Real-Time PCR System (Applied Biosystems). SYBR green reagent (Applied Biosystems) was used to quantitate mRNA for $p14^{ARF}$, $p16^{INK4A}$ and β-actin as described.[13,35,63] The relative level of each mRNA was normalized to β-actin as an internal control. The following primer sequences were used for RT–PCR to determine HPV E6 (E6 forward; 5′-TCAGGACCCACAGGAGCGACC-3′; E6 reverse; 5′-TCGACCGGTCCACCGACCC-3′) and E7 (E7 forward; 5′-ATG CATGGAGATACACCTACATTGC-3′; E7 reverse; 5′-CATTAACAGGTCTTCCAA AGTACGAATG-3′).

Western blotting analysis

Whole-cell lysates were prepared as described.[13,35] Twenty micrograms of denatured protein was fractionated on a NuPAGE Bis-Tris 4–12% gel (Invitrogen). Following electrotransfer, Immobilon-P membranes (Millipore, Billerica, MA, USA) were incubated with primary antibodies for Notch1 (1:1000 rat monoclonal 5B5; Cell Signaling), $ICN1^{Val1744}$ (1:1000 rabbit monoclonal anti-cleaved NOTCH1 Val1744 D3B8; Cell Signaling), ICN3 (1:1000 rat monoclonal anti-NOTCH3 8G5; Cell Signaling), JAG1 (1:1000 rabbit monoclonal anti-Jagged1 28H8; Cell Signaling), pRb (1:1000 rabbit polyclonal anti-Phospho-Rb Ser^{780}; Cell Signaling), p16 (1:1000 mouse monoclonal anti-Human p16 G175–1239; BD Biosciences), p15 (1:200 mouse monoclonal anti-p15 15P06; Santa Cruz Biotechnology, Santa Cruz, CA, USA), p21 (1:1000 mouse monoclonal anti-Human Cip1; BD Biosciences), p53 (1:1000 Rabbit polyclonal anti-p53; Cell Signaling) IVL (1:1000 mouse monoclonal anti-Involucrin clone SY5; Sigma-Aldrich, St Louis, MO, USA), β-actin (1:30 000 mouse monoclonal anti-β-actin AC-74; Sigma-Aldrich), Cat. no. A5316, and then with the appropriate horseradish peroxidase-conjugated secondary antibody (GE Healthcare, Piscataway, NJ, USA). β-Actin served as a loading control.

Soft agar colony-formation assays

Soft agar colony-formation assays were done as described.[35] In brief, 1×10^3 cells were suspended in 0.67% agarose containing media and overlaid on top of a 1% agarose per well (24-well plate). Two hundred microliters of medium with or without 1 μg/ml DOX was added twice a week in each well and grown for 3 weeks. Colonies >100 μm were counted following Giemsa staining.

Xenograft transplantation experiments and histopathological analysis

Xenograft transplantation experiments were done as described.[35] In brief, 5×10^6 cells were suspended in 50% Matrigel and implanted subcutaneously into the dorsal skin of athymic *nu/nu* mice (4–6 weeks old) (Charles River Laboratories, Wilmington, MA, USA). Tumor growth was monitored, and histopathological analysis was done as described.[13] Immunohistochemistry was done using primary antibodies for Notch1 (polyclonal anti-NOTCH1 ab27526; 1:500 at 4 °C overnight with sections microwaved at pH3.0) (Abcam, Cambridge, MA, USA), Ki67 (Rabbit monoclonal anti-Ki67 ab16667; 1:200 at 4 °C overnight with sections microwaved at pH6.0; Abcam), Caspase3 (Rabbit monoclonal anti Cleaved Caspase-3 Asp175 5A1E 9664; 1:800 at 4 °C overnight with sections microwaved at pH6.0; Cell Signaling). Signals were developed using the diaminobenzidine substrate kit (Vector Laboratories, Burlingame, CA, USA) following incubation with secondary anti-mouse immunoglobulin G (Vector; 1:100 at 37 °C for 30 min) or anti-rabbit immunoglobulin G (Vector; 1:200 at 37 °C for 30 min) and counter-stained with hematoxylin (Thermo Fisher Scientific, Hampton, NH, USA, CS401-1D). Stained objects were captured with a Nikon Microphot microscope (Nikon) and imaged with a digital camera. Immunohistochemical staining was assessed independently (SN and AKS), and the intensity was expressed as negative (−), weakly positive (+) or moderately positive (++). All experiments were done under approved protocols from the University of Pennsylvania.

Statistical analysis

Data are presented as mean ± s.e. or mean ± s.d. and were analyzed by two-tailed Student's *t*-test. $P<0.05$ was considered significant.

CONFLICT OF INTEREST

The authors declare no conflict of interest.

ACKNOWLEDGEMENTS

We thank Dr Hiroshi Shirasawa (Chiba University, Chiba, Japan) for the gift of EN60 cells. We are grateful to the Molecular Pathology & Imaging, Molecular Biology/Gene

Expression and Cell Culture Core Facilities of the NIH/NIDDK Center for Molecular Studies in Digestive and Liver Diseases (P30-DK050306) and of the NIH P01CA098101. This study was supported in part by NIH Grants P01CA098101 (to SK, MN, KAW, DB, HK, SN, SO, PAG, AJK-S, AB, K-KW, JAD, HN and AKR), U01CA143056 (to AKR), R01DK077005 (to HN), K26 RR032714 (to HN), Pennsylvania CURE Program Grant (to HN), F32-CA174176 (to KAW), F32-DE024685 to (NF), K08DE022842, Trio/ACS Career Award and VA CPPF Grant (to DB), K07CA137140 (to AME), University of Pennsylvania University Research Foundation Award (to HN), University of Pennsylvania, Abramson Cancer Center Pilot Project Grant (to HN), and the American Cancer Society RP-10-033-01-CCE (to AKR).

REFERENCES

1 Enzinger PC, Mayer RJ. Esophageal cancer. *New Engl J Med* 2003; **349**: 2241–2252.
2 Nakagawa H, Katzka D, Rustgi AK. Biology of esophageal cancer. In: Rustgi AK (ed). *Gastrointestinal Cancers*. Elsevier: London, UK, 2003, pp 241–251.
3 Harada H, Nakagawa H, Oyama K, Takaoka M, Andl CD, Jacobmeier B *et al.* Telomerase induces immortalization of human esophageal keratinocytes without p16INK4a inactivation. *Mol Cancer Res* 2003; **1**: 729–738.
4 Sashiyama H, Shino Y, Kawamata Y, Tomita Y, Ogawa N, Shimada H *et al.* Immortalization of human esophageal keratinocytes by E6 and E7 of human papillomavirus type 16. *Int J Oncol* 2001; **19**: 97–103.
5 Takaoka M, Harada H, Deramaudt TB, Oyama K, Andl CD, Johnstone CN *et al.* Ha-Ras(G12V) induces senescence in primary and immortalized human esophageal keratinocytes with p53 dysfunction. *Oncogene* 2004; **23**: 6760–6768.
6 Oyama K, Okawa T, Nakagawa H, Takaoka M, Andl CD, Kim SH *et al.* AKT induces senescence in primary esophageal epithelial cells but is permissive for differentiation as revealed in organotypic culture. *Oncogene* 2007; **26**: 2353–2364.
7 Ohashi S, Natsuizaka M, Wong GS, Michaylira CZ, Grugan KD, Stairs DB *et al.* Epidermal growth factor receptor and mutant p53 expand an esophageal cellular subpopulation capable of epithelial-to-mesenchymal transition through ZEB transcription factors. *Cancer Res* 2010; **70**: 4174–4184.
8 Okawa T, Michaylira CZ, Kalabis J, Stairs DB, Nakagawa H, Andl CD *et al.* The functional interplay between EGFR overexpression, hTERT activation, and p53 mutation in esophageal epithelial cells with activation of stromal fibroblasts induces tumor development, invasion, and differentiation. *Genes Dev* 2007; **21**: 2788–2803.
9 Kim SH, Nakagawa H, Navaraj A, Naomoto Y, Klein-Szanto AJ, Rustgi AK *et al.* Tumorigenic conversion of primary human esophageal epithelial cells using oncogene combinations in the absence of exogenous Ras. *Cancer Res* 2006; **66**: 10415–10424.
10 McElhinny AS, Li JL, Wu L. Mastermind-like transcriptional co-activators: emerging roles in regulating cross talk among multiple signaling pathways. *Oncogene* 2008; **27**: 5138–5147.
11 Blanpain C, Lowry WE, Pasolli HA, Fuchs E. Canonical notch signaling functions as a commitment switch in the epidermal lineage. *Genes Dev* 2006; **20**: 3022–3035.
12 Rangarajan A, Talora C, Okuyama R, Nicolas M, Mammucari C, Oh H *et al.* Notch signaling is a direct determinant of keratinocyte growth arrest and entry into differentiation. *EMBO J* 2001; **20**: 3427–3436.
13 Ohashi S, Natsuizaka M, Yashiro-Ohtani Y, Kalman RA, Nakagawa M, Wu L *et al.* NOTCH1 and NOTCH3 coordinate esophageal squamous differentiation through a CSL-dependent transcriptional network. *Gastroenterology* 2010; **139**: 2113–2123.
14 Ranganathan P, Weaver KL, Capobianco AJ. Notch signalling in solid tumours: a little bit of everything but not all the time. *Nat Rev Cancer* 2011; **11**: 338–351.
15 Hijioka H, Setoguchi T, Miyawaki A, Gao H, Ishida T, Komiya S *et al.* Upregulation of Notch pathway molecules in oral squamous cell carcinoma. *Int J Oncol* 2010; **36**: 817–822.
16 Zagouras P, Stifani S, Blaumueller CM, Carcangiu ML, Artavanis-Tsakonas S. Alterations in Notch signaling in neoplastic lesions of the human cervix. *Proc Natl Acad Sci USA* 1995; **92**: 6414–6418.
17 Rangarajan A, Syal R, Selvarajah S, Chakrabarti O, Sarin A, Krishna S. Activated Notch1 signaling cooperates with papillomavirus oncogenes in transformation and generates resistance to apoptosis on matrix withdrawal through PKB/Akt. *Virology* 2001; **286**: 23–30.
18 Weijzen S, Zlobin A, Braid M, Miele L, Kast WM. HPV16 E6 and E7 oncoproteins regulate Notch-1 expression and cooperate to induce transformation. *J Cell Physiol* 2003; **194**: 356–362.
19 Talora C, Sgroi DC, Crum CP, Dotto GP. Specific down-modulation of Notch1 signaling in cervical cancer cells is required for sustained HPV-E6/E7 expression and late steps of malignant transformation. *Genes Dev* 2002; **16**: 2252–2263.
20 Agrawal N, Frederick MJ, Pickering CR, Bettegowda C, Chang K, Li RJ *et al.* Exome sequencing of head and neck squamous cell carcinoma reveals inactivating mutations in NOTCH1. *Science* 2011; **333**: 1154–1157.
21 Stransky N, Egloff AM, Tward AD, Kostic AD, Cibulskis K, Sivachenko A *et al.* The mutational landscape of head and neck squamous cell carcinoma. *Science* 2011; **333**: 1157–1160.
22 Wang NJ, Sanborn Z, Arnett KL, Bayston LJ, Liao W, Proby CM *et al.* Loss-of-function mutations in Notch receptors in cutaneous and lung squamous cell carcinoma. *Proc Natl Acad Sci USA* 2011; **108**: 17761–17766.
23 Agrawal N, Jiao Y, Bettegowda C, Hutfless SM, Wang Y, David S *et al.* Comparative genomic analysis of esophageal adenocarcinoma and squamous cell carcinoma. *Cancer Discov* 2012; **2**: 899–905.
24 Lefort K, Mandinova A, Ostano P, Kolev V, Calpini V, Kolfschoten I *et al.* Notch1 is a p53 target gene involved in human keratinocyte tumor suppression through negative regulation of ROCK1/2 and MRCKalpha kinases. *Genes Dev* 2007; **21**: 562–577.
25 Li T, Wen H, Brayton C, Laird FM, Ma G, Peng S *et al.* Moderate reduction of gamma-secretase attenuates amyloid burden and limits mechanism-based liabilities. *J Neurosci* 2007; **27**: 10849–10859.
26 Nicolas M, Wolfer A, Raj K, Kummer JA, Mill P, van Noort M *et al.* Notch1 functions as a tumor suppressor in mouse skin. *Nat Genet* 2003; **33**: 416–421.
27 Pan Y, Lin MH, Tian X, Cheng HT, Gridley T, Shen J *et al.* gamma-secretase functions through Notch signaling to maintain skin appendages but is not required for their patterning or initial morphogenesis. *Dev Cell* 2004; **7**: 731–743.
28 Proweller A, Tu L, Lepore JJ, Cheng L, Lu MM, Seykora J *et al.* Impaired notch signaling promotes de novo squamous cell carcinoma formation. *Cancer Res* 2006; **66**: 7438–7444.
29 Zhang YW, Wang R, Liu Q, Zhang H, Liao FF, Xu H. Presenilin/gamma-secretase-dependent processing of beta-amyloid precursor protein regulates EGF receptor expression. *Proc Natl Acad Sci USA* 2007; **104**: 10613–10618.
30 Demehri S, Turkoz A, Kopan R. Epidermal Notch1 loss promotes skin tumorigenesis by impacting the stromal microenvironment. *Cancer Cell* 2009; **16**: 55–66.
31 Venkatesh D, Fredette N, Rostama B, Tang Y, Vary CP, Liaw L *et al.* RhoA-mediated signaling in Notch-induced senescence-like growth arrest and endothelial barrier dysfunction. *Arterioscler Thromb Vasc Biol* 2011; **31**: 876–882.
32 Liu ZJ, Tan Y, Beecham GW, Seo DM, Tian R, Li Y *et al.* Notch activation induces endothelial cell senescence and pro-inflammatory response: implication of Notch signaling in atherosclerosis. *Atherosclerosis* 2012; **225**: 296–303.
33 Lowell S, Jones P, Le Roux I, Dunne J, Watt FM. Stimulation of human epidermal differentiation by delta-notch signalling at the boundaries of stem-cell clusters. *Curr Biol* 2000; **10**: 491–500.
34 Dickson MA, Hahn WC, Ino Y, Ronfard V, Wu JY, Weinberg RA *et al.* Human keratinocytes that express hTERT and also bypass a p16(INK4a)-enforced mechanism that limits life span become immortal yet retain normal growth and differentiation characteristics. *Mol Cell Biol* 2000; **20**: 1436–1447.
35 Ohashi S, Natsuizaka M, Naganuma S, Kagawa S, Kimura S, Itoh H *et al.* A NOTCH3-mediated squamous cell differentiation program limits expansion of EMT-competent cells that express the ZEB transcription factors. *Cancer Res* 2011; **71**: 6836–6847.
36 Jia LQ, Osada M, Ishioka C, Gamo M, Ikawa S, Suzuki T *et al.* Screening the p53 status of human cell lines using a yeast functional assay. *Mol Carcinog* 1997; **19**: 243–253.
37 Liu Q, Yan YX, McClure M, Nakagawa H, Fujimura F, Rustgi AK. MTS-1 (CDKN2) tumor suppressor gene deletions are a frequent event in esophagus squamous cancer and pancreatic adenocarcinoma cell lines. *Oncogene* 1995; **10**: 619–622.
38 Dotto GP. Crosstalk of Notch with p53 and p63 in cancer growth control. *Nat Rev Cancer* 2009; **9**: 587–595.
39 Bertwistle D, Sugimoto M, Sherr CJ. Physical and functional interactions of the Arf tumor suppressor protein with nucleophosmin/B23. *Mol Cell Biol* 2004; **24**: 985–996.
40 Ovcharenko I, Nobrega MA, Loots GG, Stubbs L. ECR Browser: a tool for visualizing and accessing data from comparisons of multiple vertebrate genomes. *Nucleic Acids Res* 2004; **32**: W280–W286.
41 Lee DK, Kim BC, Kim IY, Cho EA, Satterwhite DJ, Kim SJ. The human papilloma virus E7 oncoprotein inhibits transforming growth factor-beta signaling by blocking binding of the Smad complex to its target sequence. *J Biol Chem* 2002; **277**: 38557–38564.
42 Zavadil J, Cermak L, Soto-Nieves N, Bottinger EP. Integration of TGF-beta/Smad and Jagged1/Notch signalling in epithelial-to-mesenchymal transition. *EMBO J* 2004; **23**: 1155–1165.
43 Bierie B, Moses HL. Tumour microenvironment: TGFbeta: the molecular Jekyll and Hyde of cancer. *Nat Rev Cancer* 2006; **6**: 506–520.
44 Natsugoe S, Xiangming C, Matsumoto M, Okumura H, Nakashima S, Sakita H *et al.* Smad4 and transforming growth factor beta1 expression in patients with squamous cell carcinoma of the esophagus. *Clin Cancer Res* 2002; **8**: 1838–1842.
45 Natsuizaka M, Ohashi S, Wong GS, Ahmadi A, Kalman RA, Budo D *et al.* Insulin-like growth factor-binding protein-3 promotes transforming growth factor-{beta}1-

mediated epithelial-to-mesenchymal transition and motility in transformed human esophageal cells. *Carcinogenesis* 2010; **31**: 1344–1353.
46 Natsuizaka M, Naganuma S, Kagawa S, Ohashi S, Ahmadi A, Subramanian H *et al.* Hypoxia induces IGFBP3 in esophageal squamous cancer cells through HIF-1alpha-mediated mRNA transcription and continuous protein synthesis. *FASEB J* 2012; **26**: 2620–2630.
47 Gustafsson MV, Zheng X, Pereira T, Gradin K, Jin S, Lundkvist J *et al.* Hypoxia requires notch signaling to maintain the undifferentiated cell state. *Dev Cell* 2005; **9**: 617–628.
48 Cui H, Kong Y, Xu M, Zhang H. Notch3 functions as a tumor suppressor by controlling cellular senescence. *Cancer Res* 2013; **73**: 3451–3459.
49 Yugawa T, Handa K, Narisawa-Saito M, Ohno S, Fujita M, Kiyono T. Regulation of Notch1 gene expression by p53 in epithelial cells. *Mol Cell Biol* 2007; **27**: 3732–3742.
50 Pascal T, Debacq-Chainiaux F, Chretien A, Bastin C, Dabee AF, Bertholet V *et al.* Comparison of replicative senescence and stress-induced premature senescence combining differential display and low-density DNA arrays. *FEBS Lett* 2005; **579**: 3651–3659.
51 Tremain R, Marko M, Kinnimulki V, Ueno H, Bottinger E, Glick A. Defects in TGF-beta signaling overcome senescence of mouse keratinocytes expressing v-Ha-ras. *Oncogene* 2000; **19**: 1698–1709.
52 Lin S, Yang J, Elkahloun AG, Bandyopadhyay A, Wang L, Cornell JE *et al.* Attenuation of TGF-beta signaling suppresses premature senescence in a p21-dependent manner and promotes oncogenic Ras-mediated metastatic transformation in human mammary epithelial cells. *Mol Biol Cell* 2012; **23**: 1569–1581.
53 Kolev V, Mandinova A, Guinea-Viniegra J, Hu B, Lefort K, Lambertini C *et al.* EGFR signalling as a negative regulator of Notch1 gene transcription and function in proliferating keratinocytes and cancer. *Nat Cell Biol* 2008; **10**: 902–911.
54 Kuilman T, Michaloglou C, Mooi WJ, Peeper DS. The essence of senescence. *Genes Dev* 2010; **24**: 2463–2479.
55 Thiery JP, Acloque H, Huang RY, Nieto MA. Epithelial-mesenchymal transitions in development and disease. *Cell* 2009; **139**: 871–890.
56 Ansieau S, Bastid J, Doreau A, Morel AP, Bouchet BP, Thomas C *et al.* Induction of EMT by twist proteins as a collateral effect of tumor-promoting inactivation of premature senescence. *Cancer Cell* 2008; **14**: 79–89.
57 Pickering CR, Zhang J, Yoo SY, Bengtsson L, Moorthy S, Neskey DM *et al.* Integrative genomic characterization of oral squamous cell carcinoma identifies frequent somatic drivers. *Cancer Discov* 2013; **3**: 770–781.
58 Ling H, Sylvestre JR, Jolicoeur P. Cyclin D1-dependent induction of luminal inflammatory breast tumors by activated Notch3. *Cancer Res* 2013; **73**: 5963–5973.
59 Aster JC, Xu L, Karnell FG, Patriub V, Pui JC, Pear WS. Essential roles for ankyrin repeat and transactivation domains in induction of T-cell leukemia by notch1. *Mol Cell Biol* 2000; **20**: 7505–7515.
60 Jeffries S, Capobianco AJ. Neoplastic transformation by Notch requires nuclear localization. *Mol Cell Biol* 2000; **20**: 3928–3941.
61 Wrana JL, Attisano L, Carcamo J, Zentella A, Doody J, Laiho M *et al.* TGF beta signals through a heteromeric protein kinase receptor complex. *Cell* 1992; **71**: 1003–1014.
62 Mroz EA, Baird AH, Michaud WA, Rocco JW. COOH-terminal binding protein regulates expression of the p16INK4A tumor suppressor and senescence in primary human cells. *Cancer Res* 2008; **68**: 6049–6053.
63 Maruo S, Zhao B, Johannsen E, Kieff E, Zou J, Takada K. Epstein-Barr virus nuclear antigens 3C and 3A maintain lymphoblastoid cell growth by repressing p16INK4A and p14ARF expression. *Proc Natl Acad Sci USA* 2011; **108**: 1919–1924.
64 Cordenonsi M, Dupont S, Maretto S, Insinga A, Imbriano C, Piccolo S. Links between tumor suppressors: p53 is required for TGF-beta gene responses by cooperating with Smads. *Cell* 2003; **113**: 301–314.
65 Young AR, Narita M, Ferreira M, Kirschner K, Sadaie M, Darot JF *et al.* Autophagy mediates the mitotic senescence transition. *Genes Dev* 2009; **23**: 798–803.
66 Lee BY, Han JA, Im JS, Morrone A, Johung K, Goodwin EC *et al.* Senescence-associated beta-galactosidase is lysosomal beta-galactosidase. *Aging Cell* 2006; **5**: 187–195.
67 Kurz DJ, Decary S, Hong Y, Erusalimsky JD. Senescence-associated (beta)-galactosidase reflects an increase in lysosomal mass during replicative ageing of human endothelial cells. *J Cell Sci* 2000; **113**(Pt 20): 3613–3622.

Supplementary Information accompanies this paper on the Oncogene website (http://www.nature.com/onc)

Hepatology Research

Hepatology Research 2014 doi: 10.1111/hepr.12421

Original Article

Serum granulysin levels as a predictor of serious telaprevir-induced dermatological reactions

Goki Suda,[1] Yoshiya Yamamoto,[2] Astushi Nagasaka,[3] Ken Furuya,[4] Mineo Kudo,[5] Yoshimichi Chuganji,[6] Yoko Tsukuda,[1] Seiji Tsunematsu,[1] Fumiyuki Sato,[1] Katsumi Terasita,[1] Masato Nakai,[1] Hiromasa Horimoto,[1] Takuya Sho,[1] Mitsuteru Natsuizaka,[1] Kouji Ogawa,[1] Shunsuke Ohnishi,[1] Makoto Chuma,[1] Yasuyuki Fujita,[7] Riichiro Abe,[7] Miki Taniguchi,[8] Mina Nakagawa,[8] Yasuhiro Asahina[8] and Naoya Sakamoto[1] for the NORTE Study Group

[1]*Department of Gastroenterology and Hepatology, Graduate School of Medicine, Hokkaido University,* [2]*Hakodate City Hospital,* [3]*Sapporo City General Hospital,* [4]*Hokkaido Social Insurance Hospital,* [5]*Sapporo Hokuyu Hospital,* [7]*Department of Dermatology, Hokkaido University Graduate School of Medicine, Hokkaido,* [6]*Tokyo Metropolitan Bokuto Hospital, and* [8]*Department of Gastroenterology and Hepatology, Tokyo Medical and Dental University, Tokyo, Japan*

Aim: Telaprevir-based therapy for chronic hepatitis C patients is effective; however, the high prevalence of dermatological reactions is an outstanding issue. The mechanism and characteristics of such adverse reactions are unclear; moreover, predictive factors remain unknown. Granulysin was recently reported to be upregulated in the blisters of patients with Stevens–Johnson syndrome (SJS). Therefore, we investigated the risk factors for severe telaprevir-induced dermatological reactions as well as the association between serum granulysin levels and the severity of such reactions.

Methods: A total of 89 patients who received telaprevir-based therapy and had complete clinical information were analyzed. We analyzed the associations between dermatological reactions and clinical factors. Next, we investigated the time-dependent changes in serum granulysin levels in five and 14 patients with grade 3 and non-grade 3 dermatological reactions, respectively.

Results: Of the 89 patients, 57 patients had dermatological reactions, including nine patients with grade 3. Univariate analysis revealed that grade 3 dermatological reactions were significantly associated with male sex. Moreover, serum granulysin levels were significantly associated with the severity of dermatological reactions. Three patients with grade 3 dermatological reaction had severe systemic manifestations including SJS, drug-induced hypersensitivity syndrome, and systemic lymphoid swelling and high-grade fever; all were hospitalized. Importantly, among the three patients, two patients' serum granulysin levels exceeded 8 ng/mL at onset and symptoms deteriorated within 6 days.

Conclusion: Male patients are at high risk for severe telaprevir-induced dermatological reactions. Moreover, serum granulysin levels are significantly associated with the severity of dermatological reactions and may be a predictive factor in patients treated with telaprevir-based therapy.

Key words: drug-induced hypersensitivity syndrome, granulysin, hepatitis C virus, telaprevir, toxic epidermal necrolysis

INTRODUCTION

HEPATITIS C IS a major pathogen causing liver cirrhosis and hepatocellular carcinoma worldwide. Until recently, standard therapies for chronic hepatitis C virus (HCV) genotype 1 infection were based on the combination of pegylated interferon (PEG IFN) and ribavirin (RBV); these combination therapies yield a sustained virological response (SVR) rate of approximately 50%.[1] Several classes of novel direct-acting antivirals

Correspondence: Dr Goki Suda, Department of Gastroenterology and Hepatology/Graduate School of Medicine, Hokkaido University, North 15, West 7, Kita-ku, Sapporo, Hokkaido 060-8638, Japan. Email: gsudgast@pop.med.hokudai.ac.jp

Conflict of interest: The authors declare that they have nothing to disclose regarding funding from the industry or conflicts of interest with respect to the manuscript.

Received 9 June 2014; revision 27 August 2014; accepted 4 September 2014.

(DAA) were recently developed and tested in clinical trials. Two first-generation HCV NS3/4A protease inhibitors, boceprevir[2,3] and telaprevir,[4–6] have been approved for the treatment of genotype 1 HCV infection. The inclusion of these agents in HCV treatment regimens has led to large improvements in treatment success rates.

Telaprevir, the first DAA, is administrated in combination with PEG IFN and RBV for 24 weeks, resulting in SVR rates up to 70–80%.[4,6–8] Although the telaprevir combination regimen is highly effective, the high frequency and severity of adverse events are outstanding issues limiting its use. Dermatological reactions are particularly prevalent, developing in 56–84.6% of patients treated with telaprevir, PEG IFN and RBV combination therapy.[9,10] Moreover, the prevalence of severe dermatological reactions including Stevens–Johnson syndrome/toxic epidermal necrolysis (SJS/TEN) and drug-induced hypersensitivity syndrome (DIHS) are substantially higher in patients treated with telaprevir-based therapy than PEG IFN and RBV combination therapy.[8,10] McHutchison *et al.* reported that 7% of patients treated with telaprevir, PEG IFN and RBV combination therapy discontinue therapy because of rash or pruritus in contrast to only 1% of patients treated with PEG IFN and RBV.[8] In some patients, serious skin reactions persist even after stopping all drugs.[10] However, the pathogenesis and clinical predictors of these adverse reactions are poorly understood.

Granulysin is a 15-kDa cationic cytolytic protein released by cytotoxic T lymphocytes and natural killer cells that induces apoptosis in target cells and has antimicrobial activities.[11] Serum levels of granulysin are elevated in primary virus infections including Epstein–Barr virus and parvovirus B19.[12] It was recently reported that serum granulysin levels are significantly elevated in patients with several types of severe dermatological lesions including SJS/TEN, which is the characteristic serious adverse event in telaprevir-containing regimens.[13,14]

Accordingly, the present study determined the risk factors for severe dermatological reactions in patients receiving telaprevir, PEG IFN and RBV combination therapy as well as the association between serum levels of granulysin and severe dermatological reactions.

METHODS

Patients and methods

IN THIS RETROSPECTIVE case–control study, at Hokkaido University Hospital and associated hospitals in the NORTE Study Group, between December 2011 and November 2013, a total of 123 patients positive for HCV genotype 1 with high serum HCV RNA titer (>5 log IU/mL) received PEG IFN, RBV and telaprevir combination therapy. Patients were excluded if they required hemodialysis or had a positive test result for serum hepatitis B surface antigen, co-infection with other HCV genotypes or HIV, evidence of autoimmune hepatitis or alcoholic hepatitis, or malignancy. Serum granulysin levels were analyzed in five healthy volunteers with no HCV, HIV or hepatitis B virus infection or any inflammatory diseases.

Written informed consent according to the process approved by the hospital's ethics committee was obtained from each patient. The study protocol conformed to the ethical guidelines of the Declaration of Helsinki and was approved by the ethics committee of each participating hospital.

Study design and treatment regimen

Telaprevir 500 or 750 mg was typically administrated every 8 h after meals for 12 weeks. PEG IFN-α-2b (PegIntron; MSD, Tokyo, Japan) 1.5 IU/kg was administrated s.c. once per week for 24 weeks. RBV (Rebetol; MSD) was administrated for 24 weeks in two divided daily doses according to bodyweight: 600, 800 and 1000 mg for patients with bodyweights of less than 60, 60–80 and more than 80 kg, respectively. The doses of PEG IFN-α-2b, RBV and telaprevir were reduced at the attending physician's discretion on the basis of hemoglobin levels, decreased white blood cell or platelet counts, or adverse events.

During treatment, patients were assessed as outpatients at weeks 1, 2, 4, 6 and 8, and then every 4 weeks thereafter for the duration of treatment. Physical examinations and blood tests were performed at all time points.

Outcomes

The primary end-point was SVR, which was defined as undetectable serum HCV RNA at 24 weeks after the end of treatment. The secondary end-points were end-of-treatment virological responses (HCV RNA undetectable in serum) and rapid virological response (RVR), which was defined as undetectable serum HCV RNA at 4 weeks after the start of treatment. Dermatological reactions were classified according to severity in the same manner as in phase III trials in Japan.[10]

Serum granulysin measurement

To evaluate serum granulysin levels in chronic hepatitis C, we first measured serum granulysin levels in five

healthy volunteers and compared them with those of 20 chronic hepatitis C patients before treatment. Serum granulysin levels were measured at the onset of dermatological reactions (within 3 days of onset); if the symptoms worsened, the time when worsening occurred was adopted. Meanwhile, in patients with no dermatological reactions, the highest serum granulysin level during treatment was adopted.

Serum granulysin levels were measured by a sandwich enzyme-linked immunosorbent assay as described previously.[12,14,15] Briefly, plates coated with 5 mg/mL mouse antibody against human granulysin, RB1 antibody, were washed with phosphate-buffered saline containing 0.1% Tween-20. Next, they were blocked with 10% fetal bovine serum in washing buffer at room temperature for 2 h. The samples and standards (Recombinant Granulysin; R&D Systems, Minneapolis, MN, USA) were incubated for 2 h at room temperature. Next, they were reacted with 0.1 mg/mL biotinylated mouse antibody against human granulysin, RC8 antibody. The plates were subsequently treated with horseradish peroxidase-conjugated streptavidin (Roche Diagnostics, Basel, Switzerland). The plates were then incubated with tetramethyl-benzidine substrate (Sigma, St Louis, MO, USA), and 1 M sulfuric acid was then added. The optical density was measured at 450 nm using a microplate reader.

Diagnosis of dermatological reactions

Dermatological reactions were investigated throughout the 24-week administration period in the telaprevir-based combination therapy. Dermatological reactions were classified according to severity as follows. Grade 1 was defined as involvement of less than 50% of the body surface and no evidence of systemic symptoms. Grade 2 was defined as involvement of less than 50% of the body surface but with multiple or diffuse lesions or rashes with characteristic mild systemic symptoms or mucous membrane involvement with no ulceration/erosion. Grade 3 was defined as a generalized rash involving 50% or more of the body surface or a rash with any new significant systemic symptoms and considered to be related to the onset and/or progression of the rash. Life-threatening reactions included SJS, TEN, drug rash with eosinophilia and systemic symptoms (DRESS)/DIHS, erythema multiforme and other life-threatening symptoms, or patients presenting with features of serious disease.

When adverse skin reactions were detected, the attending physician classified the degree of severity and referred the patients to a dermatologist as needed. In principal, when grade 3 dermatological reactions occurred, the attending physician referred the patient to a dermatologist and discontinued telaprevir. When severe dermatological reactions including SJS/TEN and DRESS/DIHS were suspected, all drugs were discontinued immediately. SJS/TEN and DIHS were diagnosed by skin biopsy and according to disease criteria, respectively.

Statistical analysis

Categorical and continuous variables were analyzed by the χ^2-test and the unpaired Mann–Whitney *U*-test, respectively. All *P*-values were two-tailed, and the level of significance was set at $P < 0.05$. Multivariate logistic regression analysis with stepwise forward selection included variables showing $P < 0.05$ in univariate analyses.

The association between dermatological reactions and serum granulysin levels were evaluated by one-way ANOVA followed by Tukey's honestly significant difference test. All statistical analyses were performed using SPSS version 21.0 (IBM Japan, Tokyo, Japan).

RESULTS

Patients

WE INCLUDED 123 chronic hepatitis C patients who received telaprevir-based triple therapy. Of these, 89 patients who had proper information of dermatological adverse events were included. The baseline characteristics of patients are shown in Table 1.

Of these 89 patients, time-dependent changes of serum granulysin concentrations were measured in 20 who had had conserved serum, at least, at the pretreatment point, 1 and 2 weeks after commencement of therapy, 1 and 2 months after commencement of therapy, the onset point of dermatological adverse reaction and the worsening point if symptoms became worse.

Among the 89 patients, 64% (57/89) developed dermatological reactions, including nine with grade 3 reactions (Table 2). The characteristics of dermatological reactions by grade are shown in Table 2. Non-grade 3 dermatological reactions tended to occur early during treatment compared to grade 3 dermatological reactions.

Association between dermatological reactions and treatment outcomes

First, we determined whether dermatological reactions were associated with final treatment outcomes.

Table 1 Baseline characteristics of the participating patients

Total number	89
HCV genotype 1b (1b/others)	89/0
Age (years)†	60.0 (19–73)
Sex (male/female)	48/41
Bodyweight (kg)†	63.0 (32–97)
Baseline white blood cell count (/μL)†	4800 (1500–9800)
Baseline hemoglobin level (g/dL)†	13.5 (9.9–16.7)
Baseline platelet count ($\times 10^3$)†	15.9 (6.6–86)
Baseline ALT level (IU/L)†	40 (15–300)
Baseline HCV RNA level ($\log^{10}$ IU/mL)†	6.5 (3.2–7.6)
Initial telaprevir dose (1500/2250 mg)	20/89
Initial PEG IFN dose (1.5/<1.5 μg/kg)	775/14
Initial RBV dose (mg/kg)†	9.8 (2.2–15.5)
IL28B gene (rs8099917) (TT/non-TT/ ND)	51/22/16
HCV 70 core mutation (wild/mutant/ND)	43/24/22
Previous treatment (naïve/relapse/NVR)	40/38/11

†Data are shown as median (range) values.
ALT, alanine transaminase; HCV, hepatitis C virus; IL28B, interleukin 28B; ND, not done; PEG IFN, pegylated interferon; RBV, ribavirin.

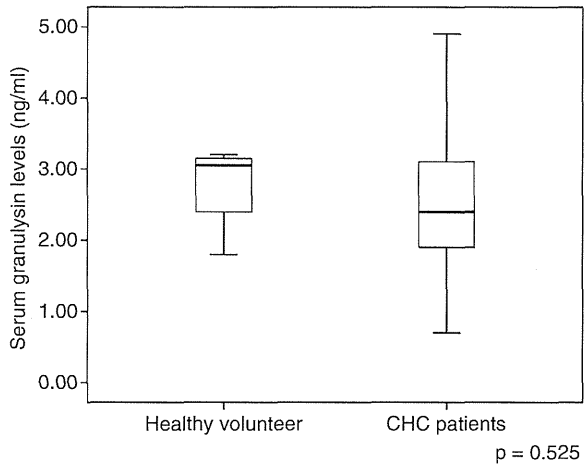

Figure 1 Serum granulysin levels of healthy volunteers and chronic hepatitis C patients. Serum granulysin levels were compared between five healthy volunteers and untreated 20 chronic hepatitis C patients. $P < 0.05$, Mann–Whitney *U*-test.

Univariate analyses identified baseline white blood cell and platelet counts, RVR, and non-grade 3 dermatological reactions significantly associated with SVR (Table 3). Among the nine patients with grade 3 dermatological reactions, three discontinued all treatment and six discontinued telaprevir administration; SVR was achieved in zero of the three (0%) and two of the six (33%), respectively.

Multivariate analysis showed that RVR and non-grade 3 dermatological reactions were significantly associated with SVR (Table 3).

Analysis of risk factors for telaprevir-induced dermatological reactions

Next, we analyzed the association between severe (i.e. grade 3) dermatological reactions and clinical parameters (Table 4). Univariate analysis showed that only sex was significantly associated with the grade 3 dermatological reactions ($P = 0.03$).

Serum granulysin levels in healthy subjects and chronic hepatitis C patients

As shown in Figure 1, serum granulysin levels did not differ significantly between healthy volunteers and chronic hepatitis C patients. Next, we evaluated the association between the severity of dermatological reactions and serum peak granulysin levels in 20 patients including five, four, five and six with grades 1, 2 and 3, and no dermatological events, respectively. One-way ANOVA showed that serum granulysin level was significantly associated with the severity of dermatological reactions ($P = 0.036$); in addition, Tukey's honestly significant difference test revealed that the serum

Table 2 Characteristics of the patients with each dermatological adverse event grade

	n	Age†	Sex (male/female)	Initial telaprevir dose (2250/1500)	Onset of DAR (days)
No DAR	32	61 (28–72)	15/17	26/6	
Grade 1	32	58 (19–73)	15/17	24/8	7 (3–50)
Grade 2	16	61 (44–73)	10/6	12/4	3.5 (1–56)
Grade 3	9	61 (48–65)	8/1	8/1	22 (1–60)

†Data are shown as median range) values.
DAR, dermatological adverse reaction

Table 3 Comparison of the clinical and laboratory characteristics of the patients with HCV infection based on therapeutic response

All patients	SVR	Non-SVR	Univariate analysis	Multivariate analysis		
$n = 89$	$n = 68$	$n = 21$	P	OR	95% CI	P
Age (years)†	60 (19–73)	62 (28–73)	0.402			
Sex (male/female)	37/31	11/10	0.870			
Bodyweight (kg)†	62 (39–97)	64 (32–87)	0.761			
Baseline white blood cells (/μL)†	5135 (1500–9800)	4200 (2490–7200)	0.048	0.492	(0.121–1.993)	0.320
Baseline hemoglobin level (g/dL)†	13.5 (10.5–16.7)	12.1 (9.9–15.4)	0.862			
Baseline platelet count ($\times 10^3$)†	16.7 (6.6–31.5)	12.8 (7.2–86)	0.025	0.388	(0.093–1.614)	0.193
Baseline ALT level (IU/L)†	37 (15–300)	53 (23–159)	0.070			
Baseline HCV RNA level ($\log^{10}$ IU/mL)†	6.7 (3.2–7.6)	6.4 (5.7–7.3)	0.812			
Baseline Cr level (mg/dL)	0.7 (0.5–1.3)	0.7 (0.5–0.9)	0.433			
Initial telaprevir dose (1500/2250 mg)	52/16	17/4	0.460			
Initial PEG IFN dose (1.5/<1.5 μg/kg)	58/10	17/4	0.430			
Initial RBV dose (mg/kg)†	9.9 (2.2–15.5)	9.5 (4.4–12.5)	0.546			
IL28B gene (rs8099917) (TT/non-TT/ND)	43/15/10	8/7/6	0.107			
Core 70 a.a. mutation (wild/mutant/ND)	36/16/16	7/8/6	0.108			
Previous treatment (naive/relapse/NVR)	34/28/6	6/10/5	0.095			
Rapid virological response (+/−)	60/8	10/11	<0.001	10.89	(2.838–41.83)	0.001
Grade 3 DAR (−/+)	66/2	14/7	<0.001	27.44	(3.718–202.5)	0.001

†Data are shown as median (range) values.
a.a., amino acid; ALT, alanine transaminase; CI, confidence interval; Cr, creatinine; DAR, dermatological adverse reaction; HCV, hepatitis C virus; IL28B, interleukin 28B; ND, not done; NVR, non-virological response; OR, odds ratio; PEG IFN, pegylated interferon; SVR, sustained virological response; RBV, ribavirin.

granulysin levels of patients with grade 3 dermatological reactions were significantly higher than those of patients with grade 1 or no dermatological reactions (both $P < 0.05$, Fig. 2).

Time-dependent changes in serum granulysin levels

We investigated the time-dependent changes in serum granulysin levels in five and 15 patients with grade 3 and non-grade 3 dermatological reactions, respectively (Fig. 3). Serum granulysin levels of patients with non-grade 3 dermatological reactions never exceeded 10 ng/ml. Of the five patients with grade 3 reactions, three had severe systemic manifestations that necessitated hospital admission: one each had SJS, DIHS, and systemic lymphoid swelling and high fever (>39 °C). All patients with grade 3 dermatological reactions with systemic manifestations had peak serum granulysin levels exceeding 10 ng/mL; importantly, the serum granulysin levels of two patients already exceeding 8 ng/mL at the onset of the reactions worsened within 6 days.

DISCUSSION

THE PRESENT STUDY demonstrates a significant association between telaprevir-induced dermatological reactions and elevated serum granulysin levels for the first time. Moreover, serum granulysin levels were significantly associated with the severity of dermatological reactions. Thus, the results indicate that serum granulysin level seems to be a useful predictor of telaprevir-induced dermatological reactions. Because the emergence of grade 3 dermatological reactions was significantly associated with non-SVR (Table 3), probably associated with high rate of treatment discontinuation, it is important to predict dermatological events in the early stage to achieve good treatment outcomes.

Table 4 Comparison of the clinical and laboratory characteristics of the patients based on the presence or absence of at least a grade 3 dermatological adverse event

All patients $n = 89$	Non-grade 3 $n = 80$	Grade ≥3 $n = 9$	Univariate analysis P
Age (years)†	60 (19–73)	61 (48–65)	0.453
Sex (male/female)	40/40	8/1	0.027
Bodyweight (kg)†	62 (32–97)	64 (51–87)	0.593
Baseline white blood cell count (/μL)†	4900 (1500–9800)	4700 (3000–7000)	0.876
Baseline hemoglobin level (g/dL)†	13.5 (9.9–16.7)	14.4 (12.1–15.4)	0.196
Baseline platelet count ($\times 10^3$)†	16.0 (6.6–86.0)	13.5 (10.4–22.5)	0.605
Baseline ALT level (IU/L)†	40(15–300)	37 (23–87)	0.765
Baseline Cr level (mg/dL)	0.7 (0.5–1.3)	0.8 (0.6–0.9)	0.123
Baseline HCV RNA level ($\log^{10}$ IU/mL)†	6.6 (3.2–7.6)	6.4 (5.7–7.1)	0.465
Initial telaprevir dose (1500/2250 mg)	62/18	7/2	0.675
Initial telaprevir/bodyweight (mg/kg)	33.7 (20–71.4)	30.0 (23.6–44.1)	0.563
Initial PEG IFN dose (1.5/<1.5 μg/kg)	66/14	9/0	0.198
Initial RBV dose (mg/kg)†	9.7 (2.2–15.5)	10.7 (7.7–12.9)	0.161
IL28B gene (rs8099917) (TT/non-TT/ND)	47/19/14	4/3/2	0.353
Core 70 a.a. mutation (wild/mutant/ND)	38/22/20	5/2/2	0.511
Previous treatment (naïve/relapse/NVR)	35/36/9	5/2/2	0.972
Onset of dermatological AE (days)	5 (1–75)	22 (1–60)	0.352

†Data are shown as median (range) values.
a.a., amino acid; AE, adverse event; ALT, alanine transaminase; Cr, creatinine; HCV, hepatitis C virus; IL28B, interleukin 28B; NVR, non-virological response; PEG IFN, pegylated interferon; RBV, ribavirin.

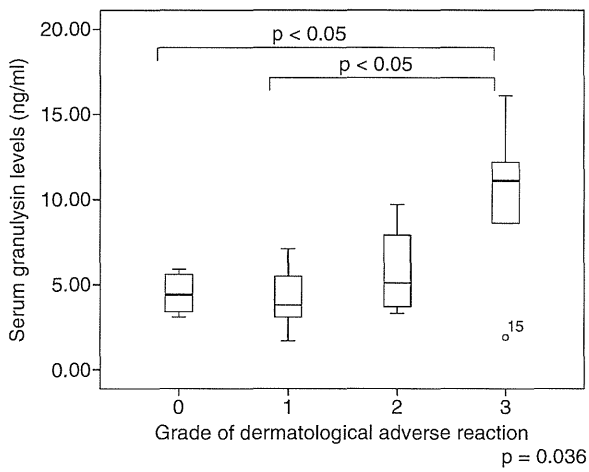

Figure 2 Association between dermatological adverse reaction severity and serum granulysin level. Serum granulysin levels were measured at the onset of dermatological reactions (i.e. within 3 days of onset); if the symptoms worsened, the time of worsening was adopted. In patients with no dermatological events, the highest serum granulysin level during treatment was adopted. $P < 0.05$, one-way ANOVA.

Recent genome-wide association studies have identified that genetic polymorphisms around the IL28B gene locus significantly associated with the outcome of PEG IFN and RBV combination therapy in HCV patients. Thus, PEG IFN and RBV combination therapy is ineffective in a subset of HCV-infected patients who have IL28B TG or GG genotypes, limiting the use of this therapy.[16] Therefore, novel drugs with different antiviral mechanisms were required. Accordingly, DAA were developed; they are mainly classified as NS3/4A protease inhibitors, or NS5B or NS5A inhibitors.[17] The NS3/4A serine protease inhibitor telaprevir, in combination with PEG IFN and RBV, has demonstrated the most promising results.[6–8] However, adverse events, especially severe dermatological reactions, develop more frequently in patients treated with telaprevir than those treated with only PEG IFN and RBV.

Little is known about the mechanisms of telaprevir-induced dermatological reactions. Reactions develop in patients treated with PEG IFN and RBV combination therapy[18,19] as well as telaprevir monotherapy.[20,21] It should be noted that the dermatological reactions in telaprevir monotherapy or PEG IFN and RBV therapy alone are generally mild.[7,8,20] However, dermatological

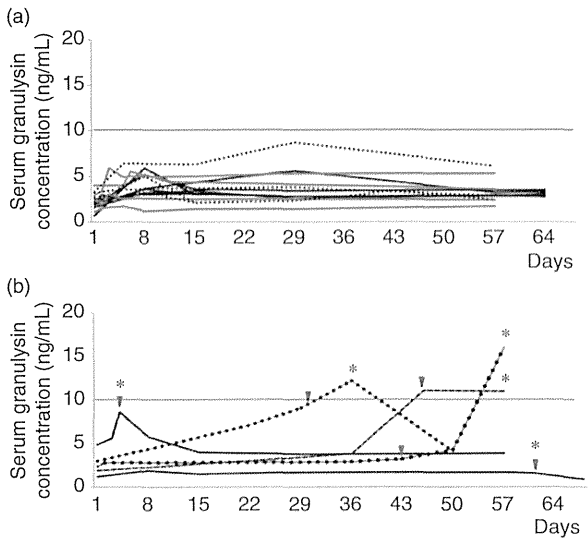

Figure 3 Association between time-dependent changes in serum granulysin levels and severe telaprevir-induced dermatological adverse reactions. (a) Time-dependent changes in serum granulysin levels patients with non-grade 3 dermatological reactions (three, five and six with grade 2, grade 1 and no reactions, respectively). The dashed line, gray line and black line indicate grade 2, grade 1 and no reaction, respectively. (b) Time-dependent changes in serum granulysin levels of five patients with grade 3 dermatological events. The dashed line indicates patients with severe systemic manifestations. Arrowheads indicate the onset of dermatological events and asterisks indicate the onset of grade 3 dermatological events.

reactions in telaprevir and PEG IFN/RBV combination therapy may be severe, indicating a synergistic effect. Severe dermatological events including SJS/TEN and DIHS have been reported in telaprevir-based triple therapy; these are life-threatening, and fatal cases have been reported.

The onset of grade 3 dermatological reactions tended to be later than non-grade 3 reactions, the same as in the study of Torii *et al.*[10] Taken together with the finding that male sex is a clinical risk factor, the results indicate that late-onset dermatological reactions in male patients treated with telaprevir-based triple therapy require more attention.

Roujeau *et al.* analyzed the risk factors for telaprevir-induced eczematous dermatitis and report that the incidence of telaprevir-related dermatitis was significantly higher age of more than 45 years, body mass index of less than 30 (kg/m^2), Caucasian ethnicity and treatment-naïve status.[9] While they analyzed the risk factors for telaprevir-induced eczematous dermatitis, the present study focused on the risk factors for severe telaprevir-induced dermatological reactions, because such reactions can affect treatment outcome (Table 2) and can be fatal. As mentioned above, male sex was significantly associated with grade 3 dermatological reactions. Sex is reported to be associated with the prevalence of some kinds of severe drug-induced dermatological events, although the underlying mechanism remains unknown.[22]

Fujita *et al.* report that serum granulysin levels are significantly elevated in SJS/TEN patients and thus may be a good predictive factor.[14] Therefore, we hypothesized that in telaprevir-based triple therapy for chronic hepatitis C patients, serum granulysin levels are associated with the severity of dermatological reactions and may thus be a predictive biomarker. However, Ogawa *et al.* report that serum granulysin levels also increase as a result of primary virus infections such as Epstein–Barr virus or parvovirus B19.[12] Thus, it remains unclear whether and how chronic viral infections, especially HCV, affect serum granulysin levels. In the present study, we compared serum granulysin levels between healthy volunteers and chronic hepatitis C patients; the results show that chronic HCV infection was not associated with serum granulysin levels (Fig. 1).

Chung *et al.* have reported that granulysin is the most highly expressed cytotoxic molecule in blisters of SJS/TEN and that massive keratinocyte death was induced by granulysin.[11] Fujita *et al.* reported that serum granulysin levels increased in the early stage of SJS/TEN caused by drugs including carbamazepine, imatinib and phenytoin.[14] Taken together with our results, we speculate that granulysin may be involved in the pathogenesis of early stage telaprevir-mediated dermatological adverse reactions possibly through induction of keratinocyte death.

Of five patients with grade 3 reactions, two patients without severe systemic manifestations did not have elevated serum granulysin of more than 10 ng/mL or did not have elevated levels before symptoms worsened. On the contrary, three patients with severe systemic manifestations had peak serum granulysin levels exceeding 10 ng/mL, and the symptoms of two patients with serum granulysin levels already exceeding 8 ng/mL at onset and within 6 days worsened. Therefore, serum granulysin tests may predict grade 3 dermatological adverse reaction with systemic manifestations. Furthermore, if serum granulysin levels elevate more than 8 ng/mL, more attention should be paid.

In Western countries, the prevalence of dermatological reactions in patients treated with telaprevir-based and

PEG IFN/RBV therapy are reported to be approximately 55% and 33%, respectively;[9,23] meanwhile, in Japanese patients, the respective rates are 74.9% and 58.7%. Moreover, approximately 4% and 9% of patients in Western and Japanese patients develop grade 3 reactions, respectively;[10] this is almost the same as that in the present study (10%). The difference may be due to genetic or ethnic variation. Therefore, genome-wide association studies may have identified a gene locus associated with telaprevir-induced severe dermatological reactions.

A limitation of this study is that the number of patients with grade 3 dermatological reactions is relatively small. However, the serum granulysin levels of patients with grade 3 dermatological reactions were significantly higher than those of other patients. Also, in two of the three patients with severe dermatological reactions, the serum granulysin level elevated before symptoms worsened, which are novel findings. Further study is required.

Triple therapy with the second-generation protease inhibitor simeprevir is reported to result in a similar prevalence of adverse reactions as PEG IFN and RBV combination therapy.[24,25] However, simeprevir is not approved worldwide. Although simeprevir-based triple therapy is effective, only 36–53% of prior non-responders achieve SVR.[24] Shimada *et al.* recently reported that by extending PEG IFN and RBV therapy from 24 to 48 weeks, telaprevir-based triple therapy improves the SVR to up to 68% in prior null responders.[26] Thus, telaprevir is a therapeutic option for prior null responders.

In conclusion, the present study suggests that male sex is a significant risk factor for severe telaprevir-induced dermatological reactions. In addition, serum granulysin levels are significantly associated with the severity of dermatological reactions and thus may be a good predictor of severe dermatological reactions with systemic manifestations in patients treated with telaprevir-based triple therapy.

ACKNOWLEDGMENTS

THIS STUDY WAS supported in part by grants from the Ministry of Education, Culture, Sports, Science and Technology of Japan, the Japan Society for the Promotion of Science, and the Ministry of Health, Labour and Welfare of Japan. The authors would like to thank all patients and their families as well as the investigators and staff of the 22 participating institutions. The principal investigators of the NORTE study sites are listed below in alphabetical order: Junichi Yoshida (Sapporo Social Insurance General Hospital), Atsushi Nagasaka (Sapporo City General Hospital), Akira Fuzinaga, Manabu Onodera (Abashiri-Kosei General Hospital), Hideaki Kikuchi, Tomofumi Atarashi (Obihiro-Kosei General Hospital), Ken Furuya (Hokkaido Social Insurance Hospital), Yukio Oohara, Sousi Kimura (National Hospital Organization Hokkaido Medical Center), Takuto Miyagihima (Kushiro Rosai Hosspital), Takashi Meguro (Hokkaido Gastroenterology Hospital), Akiyoshi Saga (Aiiku Hospital), Mineo Kudou (Sapporo Hokuyu Hospital), Jun Konno (Hakodate General Central Hospital), Kenichi Kumagaya (Hakodate Medical Association Hospital), Nobuaki Akakura (Sapporo Medical Center NTT EC), Tomoe Kobayashi (Tomakomai City Hospital), Uebayashi Minoru (Japanese Red Cross Kitami Hospital), Hiroshi Katou (Iwamizawa Municipal General Hospital), Yasuyuki Kunieda (Wakkanai City Hospital), Miki Tateyama (Tomakomai Nissho Hospital), Munenori Okamoto (Sapporo Century Hospital), Izumi Tunematsu (Touei Hospital) and Chuganji Yoshimichi (Tokyo Metropolitan Bokuto Hospital).

REFERENCES

1 Sakamoto N, Nakagawa M, Tanaka Y *et al.* Association of IL28B variants with response to pegylated-interferon alpha plus ribavirin combination therapy reveals intersubgenotypic differences between genotypes 2a and 2b. *J Med Virol* 2011; **83**: 871–8.
2 Poordad F, McCone J, Jr, Bacon BR *et al.* Boceprevir for untreated chronic HCV genotype 1 infection. *N Engl J Med* 2011; **364**: 1195–206.
3 Bacon BR, Gordon SC, Lawitz E *et al.* Boceprevir for previously treated chronic HCV genotype 1 infection. *N Engl J Med* 2011; **364**: 1207–17.
4 Zeuzem S, Andreone P, Pol S *et al.* Telaprevir for retreatment of HCV infection. *N Engl J Med* 2011; **364**: 2417–28.
5 Sherman KE, Flamm SL, Afdhal NH *et al.* Response-guided telaprevir combination treatment for hepatitis C virus infection. *N Engl J Med* 2011; **365**: 1014–24.
6 Jacobson IM, McHutchison JG, Dusheiko G *et al.* Telaprevir for previously untreated chronic hepatitis C virus infection. *N Engl J Med* 2011; **364**: 2405–16.
7 Kumada H, Toyota J, Okanoue T, Chayama K, Tsubouchi H, Hayashi N. Telaprevir with peginterferon and ribavirin for treatment-naive patients chronically infected with HCV of genotype 1 in Japan. *J Hepatol* 2012; **56**: 78–84.
8 McHutchison JG, Everson GT, Gordon SC *et al.* Telaprevir with peginterferon and ribavirin for chronic HCV genotype 1 infection. *N Engl J Med* 2009; **360**: 1827–38.
9 Roujeau JC, Mockenhaupt M, Tahan SR *et al.* Telaprevir-related dermatitis. *JAMA Dermatol* 2013; **149**: 152–8.

10 Torii H, Sueki H, Kumada H *et al.* Dermatological side-effects of telaprevir-based triple therapy for chronic hepatitis C in phase III trials in Japan. *J Dermatol* 2013; **40**: 587–95.
11 Chung WH, Hung SI, Yang JY *et al.* Granulysin is a key mediator for disseminated keratinocyte death in Stevens-Johnson syndrome and toxic epidermal necrolysis. *Nat Med* 2008; **14**: 1343–50.
12 Ogawa K, Takamori Y, Suzuki K *et al.* Granulysin in human serum as a marker of cell-mediated immunity. *Eur J Immunol* 2003; **33**: 1925–33.
13 Abe R, Yoshioka N, Murata J, Fujita Y, Shimizu H. Granulysin as a marker for early diagnosis of the Stevens-Johnson syndrome. *Ann Intern Med* 2009; **151**: 514–5.
14 Fujita Y, Yoshioka N, Abe R *et al.* Rapid immunochromatographic test for serum granulysin is useful for the prediction of Stevens-Johnson syndrome and toxic epidermal necrolysis. *J Am Acad Dermatol* 2011; **65**: 65–8.
15 Saigusa S, Ichikura T, Tsujimoto H *et al.* Serum granulysin level as a novel prognostic marker in patients with gastric carcinoma. *J Gastroenterol Hepatol* 2007; **22**: 1322–7.
16 Tanaka Y, Nishida N, Sugiyama M *et al.* Genome-wide association of IL28B with response to pegylated interferon-alpha and ribavirin therapy for chronic hepatitis C. *Nat Genet* 2009; **41**: 1105–9.
17 Aghemo A, De Francesco R. New horizons in hepatitis C antiviral therapy with direct-acting antivirals. *Hepatology* 2013; **58**: 428–38.
18 Lubbe J, Kerl K, Negro F, Saurat JH. Clinical and immunological features of hepatitis C treatment-associated dermatitis in 36 prospective cases. *Br J Dermatol* 2005; **153**: 1088–90.
19 Manns MP, McHutchison JG, Gordon SC *et al.* Peginterferon alfa-2b plus ribavirin compared with interferon alfa-2b plus ribavirin for initial treatment of chronic hepatitis C: a randomised trial. *Lancet* 2001; **358**: 958–65.
20 Yamada I, Suzuki F, Kamiya N *et al.* Safety, pharmacokinetics and resistant variants of telaprevir alone for 12 weeks in hepatitis C virus genotype 1b infection. *J Viral Hepat* 2012; **19**: e112–119.
21 Toyota J, Ozeki I, Karino Y *et al.* Virological response and safety of 24-week telaprevir alone in Japanese patients infected with hepatitis C virus subtype 1b. *J Viral Hepat* 2013; **20**: 167–73.
22 Bersoff-Matcha SJ, Miller WC, Aberg JA *et al.* Sex differences in nevirapine rash. *Clin Infect Dis* 2001; **32**: 124–9.
23 Cacoub P, Bourliere M, Lubbe J *et al.* Dermatological side effects of hepatitis C and its treatment: patient management in the era of direct-acting antivirals. *J Hepatol* 2012; **56**: 455–63.
24 Izumi N, Hayashi N, Kumada H *et al.* Once-daily simeprevir with peginterferon and ribavirin for treatment-experienced HCV genotype 1-infected patients in Japan: the CONCERTO-2 and CONCERTO-3 studies. *J Gastroenterol* 2014; **49**: 941–53.
25 Hayashi N, Seto C, Kato M, Komada Y, Goto S. Once-daily simeprevir (TMC435) with peginterferon/ribavirin for treatment-naive hepatitis C genotype 1-infected patients in Japan: the DRAGON study. *J Gastroenterol* 2014; **49**: 138–47.
26 Shimada N, Tsubota A, Atsukawa M *et al.* A 48-week telaprevir-based triple combination therapy improves sustained virological response rate in previous non-responders to peginterferon and ribavirin with genotype 1b chronic hepatitis C: a multicenter study. *Hepatol Res* 2014; [Epub ahead of print].

Comparison of improved prognosis between hepatitis B- and hepatitis C- related hepatocellular carcinoma.

Tatsuya Minami [1], Ryosuke Tateishi [1], Shuichiro Shiina [2], Ryo Nakagomi [1], Mayuko Kondo [1], Naoto Fujiwara[1], Shintaro Mikami [1], Masaya Sato [1], Koji Uchino [1], Kenichiro Enooku [1], Hayato Nakagawa[1], Yoshinari Asaoka [1], Yuji Kondo [1], Haruhiko Yoshida [1], Kazuhiko Koike [1]

[1] Department of Gastroenterology, Graduate School of Medicine, The University of Tokyo

[2] Department of Gastroenterology, Juntendo University

Running Title: Comparison between hepatitis B- and hepatitis C- related hepatocellular carcinoma

Corresponding Author

Ryosuke Tateishi, M.D., Ph.D.

Department of Gastroenterology

Graduate School of Medicine

The University of Tokyo

7-3-1 Hongo, Bunkyo-ku, Tokyo 113-8655, Japan

TEL +81-3-3815-5411

FAX +81-3-3814-0021

E-mail: tateishi-tky@umin.ac.jp

This article has been accepted for publication and undergone full peer review but has not been through the copyediting, typesetting, pagination and proofreading process which may lead to differences between this version and the Version of Record. Please cite this article as doi: 10.1002/hepr.12468

Word count (abstract): 246

Word count (text): 2807

Tables: 4

Figures: 2

Key words: Prognosis; hepatocellular carcinoma; hepatitis B; hepatitis C; nucleos(t)ide analogs

Abbreviations: ADV, adefovir; AFP, alpha-fetoprotein; AST, aspartate aminotransferase ; ALT, alanine aminotransferase; CI, confidence interval; DCP, des- γ -carboxy-prothrombin; ETV, entecavir; HBV, hepatitis B virus; HCC, hepatocellular carcinoma; HCV, hepatitis C virus; HR, hazard ratio; IFN, interferon; IQR, interquartile ranges; LAM, lamivudine; NA, nucleoside analogue; PEIT, percutaneous ethanol infection therapy; PMCT, percutaneous microwave coagulation therapy; PTA, percutaneous tumor ablation; RFA, radiofrequency ablation; TAE, transarterial embolization.

Funding: This work was supported by Health Sciences Research Grants of The Ministry of Health, Labour and Welfare of Japan (Research on Hepatitis). No additional external funding received for this study.
The funders had no role in study design, data collection and analysis, decision to publish, or preparation of the manuscript.